JOURNAL OF BACTERIOLOGY, Feb. 2010, p. 994–1010 Vol. 192, No. 4
0021-9193/10/$12.00 doi:10.1128/JB.01390-09

Genetic Analysis of the Regulation of Type IV Pilus Function by the Chp Chemosensory System of *Pseudomonas aeruginosa*▽

Jacob J. Bertrand,[1,4] Joyce T. West,[2,4] and Joanne N. Engel[2,3,4]*

Department of Biochemistry and Biophysics, University of California, San Francisco, California 94143[1]; Department of Medicine, University of California, San Francisco, California 94143[2]; Department of Microbiology and Immunology, University of California, San Francisco, California 94143[3]; and Microbial Pathogenesis and Host Defense Program, University of California, San Francisco, California 94143[4]

Received 22 October 2009/Accepted 1 December 2009

The virulence of the opportunistic pathogen *Pseudomonas aeruginosa* involves the coordinate expression of many virulence factors, including type IV pili, which are required for colonization of host tissues and for twitching motility. Type IV pilus function is controlled in part by the Chp chemosensory system, which includes a histidine kinase, ChpA, and two CheY-like response regulators, PilG and PilH. How the Chp components interface with the type IV pilus motor proteins PilB, PilT, and PilU is unknown. We present genetic evidence confirming the role of ChpA, PilG, and PilB in the regulation of pilus extension and the role of PilH and PilT in regulating pilus retraction. Using informative double and triple mutants, we show that (i) ChpA, PilG, and PilB function upstream of PilH, PilT, and PilU; (ii) that PilH enhances PilT function; and (iii) that PilT and PilB retain some activity in the absence of signaling input from components of the Chp system. By site-directed mutagenesis, we demonstrate that the histidine kinase domain of ChpA and the phosphoacceptor sites of both PilG and PilH are required for type IV pilus function, suggesting that they form a phosphorelay system important in the regulation of pilus extension and retraction. Finally, we present evidence suggesting that *pilA* transcription is regulated by intracellular PilA levels. We show that PilA is a negative regulator of *pilA* transcription in *P. aeruginosa* and that the Chp system functionally regulates *pilA* transcription by controlling PilA import and export.

Pseudomonas aeruginosa is a ubiquitous environmental Gram-negative bacterium that is an opportunistic human pathogen and that has been shown to infect a diverse array of eukaryotes including amoebae, nematodes, insects, plants, and mice (9, 11, 28, 49). *P. aeruginosa* is the causative agent of both acute and chronic human infections, ranging from minor skin infections to persistent and often life-threatening disease in hospitalized or immunocompromised patients such as those suffering from AIDS, extensive burns, who are undergoing chemotherapy, or those who are recovering from major surgery (39). *P. aeruginosa* also chronically infects the cystic fibrosis lung and is the primary cause of respiratory morbidity and mortality in patients with this inherited disease (39).

P. aeruginosa virulence involves the coordinate expression of a wide range of secreted and cell-associated virulence factors (17). Key among these virulence factors are the type IV pili (Tfp). Tfp are polarly localized filamentous appendages synthesized by a variety of Gram-negative bacteria, including both pathogens and environmental species such as *Myxococcus xanthus* (40). Tfp constitute the major adhesin of *P. aeruginosa* and have been shown to play a role in adherence to epithelial cells in culture and in virulence in several animal models of infection (17). Tfp also function as receptors for certain bacteriophages (6) and allow for a type of flagellum-independent surface translocation termed twitching motility (TM). TM is propelled by the coordinated extension, tethering, and retraction of Tfp (41, 47) and has been shown to be involved in complex social behaviors, such as fruiting body development in *M. xanthus* (33, 34, 59) and biofilm formation in *P. aeruginosa* (3, 7, 35, 36, 43). *P. aeruginosa* biofilms have been implicated in chronic infections (10).

The biogenesis, assembly, and function of Tfp requires more than 40 genes (40). Regulation of Tfp function is complex and involves multiple signal transduction systems, including the two-component signaling systems (*pilR*/*pilS* and *algR*/*fimS*), the global carbon metabolism regulator *crc*, the virulence factor regulator *vfr*, and a putative chemosensory system encoded by the *pilGHIJK-chpABC* gene cluster and referred to as the Chp system. The proteins encoded by these genes appear to comprise a chemosensory signal transduction pathway similar to the Che system involved in the regulation of flagellar chemotaxis in *Escherichia coli* (2, 51). As is the case with a growing number of bacterial chemotaxis systems (33, 44), regulation of Tfp function by the Chp system appears to be considerably more complex than its *E. coli* counterpart.

The core signaling components of the Chp system include a putative histidine kinase, encoded by *chpA* (55) and two CheY-like response regulators, encoded by *pilG* and *pilH* (12, 13). Previous studies have suggested that *chpA* (55) and *pilG* (12) are involved in regulating pilus extension, whereas *pilH* (13) is involved in regulating pilus retraction. Similarly, the ATPases encoded by *pilB* and *pilT* (27) are postulated to be involved in mediating pilus extension and retraction, respectively. The role of the ATPase encoded by *pilU* is unclear (8). However, due to a high degree of similarity with *pilT* and *in vitro* ATPase activ-

* Corresponding author. Mailing address: Department of Medicine, University of California, Box 0654, Rm. S380, San Francisco, CA 94143. Phone: (415) 476-7355. Fax: (415) 476-9364. E-mail: jengel@medicine.ucsf.edu.

▽ Published ahead of print on 11 December 2009.

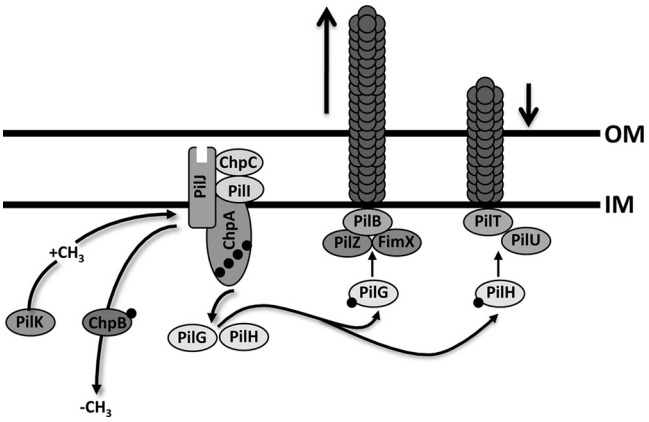

FIG. 1. Model for the regulation of type IV pilus function by the Chp chemosensory system. The hybrid histidine kinase ChpA, likely associated with the inner membrane, is coupled to a methyl-accepting chemotaxis protein receptor, PilJ, by one of two CheW adaptor protein homologues, PilI and ChpC. Upon receipt of a yet-to-be-elucidated signal, PilJ undergoes a conformational change causing ChpA to autophosphorylate. Phosphate groups are transferred from ChpA to two CheY-like response regulator proteins, PilG and PilH. PilG-P interacts with a motor complex including PilZ, the diguanylate cyclase FimX, and ATPase PilB to mediate pilus extension. PilH-P interacts with ATPases PilT and/or PilU to mediate pilus retraction. Adaptation to the chemical signal is mediated through methylation of PilJ by the competing activities of the methyltransferase PilK and the methylesterase PilB.

ity, it has been hypothesized that *pilU* may play some role in regulating pilus retraction (8, 56).

We used genetic approaches to test the hypothesis that phosphotransfer from ChpA to PilG and PilH is important for Tfp function and that PilG and PilH regulate pilus extension and retraction through PilB and PilT, respectively (Fig. 1). We demonstrate that ChpA, PilG, and PilB function upstream of PilH, PilT, and PilU and that PilH enhances PilT activity. We provide evidence that PilB and PilT retain some activity in the absence of upstream signaling input from ChpA and PilG, and PilH, respectively. We demonstrate that the histidine kinase domain of ChpA and the phosphoacceptor sites of both PilG and PilH are required for Tfp function. Finally, we present evidence suggesting that *pilA* transcription is regulated by intracellular PilA levels. We show that PilA is a negative regulator of *pilA* transcription in *P. aeruginosa* and that the Chp system functionally regulates *pilA* transcription by controlling PilA import and export.

MATERIALS AND METHODS

Bacterial strains, plasmids, and media. *Escherichia coli* strain DH5α (*recA endA gyr96 hsdR17 thi-1 supE44 relA1* ϕ80d*lacZ*ΔM15) was used in all genetic manipulations and in the preparation of DNA sequencing templates. *E. coli* strains S17.1 (*thi pro hsdR recA chr*::*RP4-2*) and SM10 (*thi thr leu tonA lacY supE recA*::*RP4-2*-Tc::Mu Km λ*pir*) were used as donor strains in bacterial conjugation. The *P. aeruginosa* strain used was PAO1 strain ATCC 15692 (American Type Culture Collection). Chemically competent *E. coli* cells (Invitrogen) were transformed according to the manufacturer's instructions. The bacterial strains and plasmids used in the present study are described in Table 1. *E. coli* and *P. aeruginosa* liquid cultures were maintained in Luria-Bertani (LB) broth, and solid medium was prepared by adding 0.8 to 1.5% agar (Bacto agar; Becton Dickinson). After mating with *E. coli*, *P. aeruginosa* strains were selected by growth on 1.5% Difco *Pseudomonas* isolation agar (Becton Dickinson). The following antibiotic concentrations were used for the selection of *E. coli*: tetracycline, 5 μg/ml; ampicillin, 100 μg/ml; gentamicin, 10 μg/ml; and kanamycin, 50 μg/ml. The following antibiotic concentrations were used for the selection of *P. aeruginosa*: tetracycline, 100 μg/ml; carbenicillin, 250 μg/ml; and gentamicin, 100 μg/ml.

Plasmid construction. All plasmids were purified by using QIAprep spin miniprep columns (Qiagen). Standard recombinant DNA manipulation techniques were used (45). Enzymes were purchased from New England Biolabs, Inc., and used as recommended by the manufacturer. All oligonucleotides used in the present study were designed based on the PAO1 genome sequence (48) and were synthesized by Qiagen or Elim Biopharmaceuticals, Inc. (Hayward, CA). The oligonucleotide primer sequences used for PCR amplification are listed in Table 2. PCR amplifications were carried out with *Pfu* Turbo DNA polymerase (Stratagene) or Herculase DNA polymerase (Stratagene), and the products were sequenced to ensure that no mutations were introduced during amplification. Intermediate cloning steps were performed using DH5α (Invitrogen). Plasmids were introduced into chemically competent *E. coli* strains.

Construction and complementation of in-frame deletion mutants. All matings were performed as described previously (55). All mutants were confirmed by Southern or PCR analysis and are listed in Table 1.

(i) ChpA. The *chpA* in-frame deletion mutant was constructed by allelic replacement and has been described previously (55). To complement the Δ*chpA* mutation, a 3′ fragment of *chpA*, including 1 kb of 3′-flanking sequence was amplified by using the chpA26.1/chpA29(Xba) PCR primer pair and cloned as an MluI/XbaI fragment into pJB219 (a modified version of pOK12 in which the KpnI and ClaI sites have been removed from the MCS) to form pJB220. A 5′ fragment of *chpA*, including 1 kb of 5′ flanking sequence was amplified by using the chpA22(HindIII)/chpA25 PCR primer pair and cloned as an HindIII/MluI fragment into pJB220 to form pJB221. Full-length *chpA* and 1 kb of 5′- and 3′-flanking sequence were subcloned as a SpeI fragment from pJB221 to pJB100 to form pJB231. pJB231 was transformed into *E. coli* S17.1, and transformants were mated to the Δ*chpA* strain to create a Δ*chpA* derivative complemented for *chpA* at its endogenous locus.

(ii) PilA. 5′ and 3′ *pilA* deletion construct fragments were amplified by using the pilA1/pilA2 and pilA3/pilA4 PCR primer pairs. An adenosine residue was added to the 3′ end of the PCR products and the modified products ligated into pGEM-T. The 5′ deletion construct was excised from pGEM-T as an NcoI/EcoRIII fragment. The 3′ deletion construct was excised from pGEM-T as an EcoRI/XbaI fragment. Excised 5′ and 3′ deletion construct fragments were concatamerized and cloned as an NcoI/XbaI fragment into pOK12. The deletion construct was excised from pOK12 as a SpeI fragment and ligated into the allelic exchange vector pJEN34 to form pJEN34PAO1KO3. pJEN34PAO1KO3 was transformed into *E. coli* S17.1, and transformants were mated to PAO1 to create an unmarked Δ*pilA* mutant. This procedure deleted amino acids 2 to 149 of the PilA protein. To complement the Δ*pilA* mutation, *pilA* and 1 kb of 5′ and 3′ flanking sequence were amplified by using the pilA1(Spe)/pilA4(Spe) PCR primer pair. The product was cloned as a SpeI fragment into pJB100 to form pJB241. pJB241 was transformed into *E. coli* S17.1, and transformants were mated to the Δ*pilA* strain to create a Δ*pilA* derivative complemented for *pilA* at its endogenous locus.

(iii) PilB. 5′ and 3′ *pilB* deletion construct fragments were amplified by using the pilB1/pilB2 and pilB3/pilB4 PCR primer pairs. PCR products were used as templates in a sequence overlap extension (SOE) reaction with the pilB1/pilB4 PCR primer pair. The SOE product was cloned as a SpeI fragment into pJB100 for form pJB122. pJB122 was transformed into *E. coli* S17.1, and transformants were mated to PAO1 to create an unmarked Δ*pilB* mutant. This procedure deleted amino acids 4 to 564 of the PilB protein. To complement the Δ*pilB* mutation, *pilB* and 1 kb of the 5′- and 3′-flanking sequence were amplified by using the pilB1/pilB4 PCR primer pair. The product was cloned as a SpeI fragment into pJB100 to form pJB246. pJB246 was transformed into *E. coli* S17.1, and transformants were mated to Δ*pilB* to create a Δ*pilB* derivative complemented for *pilB* at its endogenous locus.

(iv) PilG. 5′ and 3′ *pilG* deletion construct fragments were amplified by using the pilG1/pilG2 and pilG3/pilG4 PCR primer pairs. An adenosine residue was added to the 3′ end of the PCR products, and the modified products were ligated into pGEM-T to form pJB43 (5′ deletion construct) and pJB44 (3′ deletion construct). The 5′ deletion construct was excised from pJB43 as an EcoRI/HindIII fragment. The 3′ deletion construct was excised from pJB44 as a HindIII/XbaI fragment. Excised 5′ and 3′ deletion construct fragments were concatamerized and cloned as an EcoRI/XbaI fragment into pOK12 to form pJB60. The deletion construct was excised from pJB60 as a SpeI fragment and ligated into the allelic exchange vector pJEN34 to form pJB87. pJB87 was transformed into *E. coli* S17.1, and transformants were mated to PAO1 to create an unmarked Δ*pilG* mutant. This procedure deleted amino acids 5 to 87 of the PilG protein.

TABLE 1. Strains and plasmids used in this study

Strain or plasmid	Genotype and relevant characteristics[a]	Source or reference
Strains		
P. aeruginosa		
PAO1	Wild type	
PAO1Δ*chpA*	In-frame deletion of *chpA*	61
PAO1Δ*chpA*(comp)	PAO1Δ*chpA* complemented at the *chpA* locus	This study
PAO1Δ*fliC*	In-frame deletion of *fliC*	This study
PAO1Δ*fliC*(comp)	PAO1Δ*fliC* complemented at the *fliC* locus	This study
PAO1Δ*pilA*	In-frame deletion of *pilA*	This study
PAO1Δ*pilA*(comp)	PAO1Δ*pilA* complemented at the *pilA* locus	This study
PAO1Δ*pilB*	In-frame deletion of *pilB*	This study
PAO1Δ*pilA*(comp)	PAO1Δ*pilB* complemented at the *pilB* locus	This study
PAO1Δ*pilG*	In-frame deletion of *pilG*	This study
PAO1Δ*pilG*(comp)	PAO1Δ*pilG* complemented at the *pilG* locus	This study
PAO1Δ*pilH*	In-frame deletion of *pilH*	3
PAO1Δ*pilH*(comp)	PAO1Δ*pilH* complemented at the *pilH* locus	This study
PAO1Δ*pilR*	In-frame deletion of *pilR*	This study
PAO1Δ*pilR*(comp)	PAO1Δ*pilR* complemented at the *pilR* locus	This study
PAO1Δ$pilT^{\text{CTX-}pilU}$	In-frame deletion of *pilT*; *pilU* and 1 kb upstream sequence at *attB* site	This study
PAO1$pilT^{\text{Trunc}}$	*pilT* truncation mutant, deletes 429 bp of *pilT* including the start codon; stop codons in all three reading frames	This study
PAO1Δ*pilT*(comp)	PAO1Δ*pilT* complemented at the *pilT* locus	This study
PAO1Δ*pilU*	In-frame deletion of *pilU*	This study
PAO1Δ*pilU*(comp)	PAO1Δ*pilU* complemented at the *pilU* locus	This study
PAO1Δ*chpA*Δ*pilH*	In-frame deletion of *chpA* and *pilH*	This study
PAO1Δ*chp*Δ$pilT^{\text{CTX-}pilU}$	In-frame deletion of *chpA* and *pilT*; *pilU* and 1 kb upstream sequence at *attB* site	This study
PAO1Δ*chpA*Δ*pilU*	In-frame deletion of *chpA* and *pilU*	This study
PAO1Δ*chpA*Δ*pilT*Δ*pilU*	In-frame deletion of *chpA*, *pilT*, and *pilU*	This study
PAO1Δ*pilB*Δ*pilH*	In-frame deletion of *pilB* and *pilH*	This study
PAO1Δ*pilB*Δ$pilT^{\text{CTX-}pilU}$	In-frame deletion of *pilB* and *pilT*; *pilU* and 1 kb upstream sequence at *attB* site	This study
PAO1Δ*pilB*Δ*pilU*	In-frame deletion of *pilB* and *pilU*	This study
PAO1Δ*pilB*Δ*pilT*Δ*pilU*	In-frame deletion of *pilB*, *pilT*, and *pilU*	This study
PAO1Δ*pilG*Δ*pilH*	In-frame deletion of *pilG* and *pilH*	This study
PAO1Δ*pilG*Δ*pilT*-gent	PAO1Δ*pilG* with a Gm^r-tagged insertion in *pilT*	This study
PAO1Δ*pilG*Δ$pilT^{\text{CTX-}pilU}$	In-frame deletion of *pilG* and *pilT*; *pilU* and 1 kb upstream sequence at *attB* site	This study
PAO1Δ*pilG*Δ*pilU*-gent	PAO1Δ*pilG* with a Gm^r-tagged insertion in *pilU*	This study
PAO1Δ*pilG*Δ*pilU*	In-frame deletion of *pilG* and *pilU*	This study
PAO1Δ*pilG*Δ*pilT*Δ*pilU*	In-frame deletion of *pilG*, *pilT*, and *pilU*	This study
PAO1Δ*pilH*Δ$pilT^{\text{CTX-}pilU}$	In-frame deletion of *pilH* and *pilT*; *pilU* and 1 kb upstream sequence at *attB* site	This study
PAO1Δ*pilT*Δ*pilU*	In-frame deletion of *pilT* and *pilU*	This study
PAO1Δ*pilH*Δ*pilU*	In-frame deletion of *pilH* and *pilU*	This study
PAO1Δ*pilH*Δ*pilT*Δ*pilU*	In-frame deletion of *pilH*, *pilT*, and *pilU*	This study
PAO1*chpA*-FLAG	*chpA* with a double FLAG tag inserted into the NotI/KpnI sites of *chpA* at the *chpA* locus	This study
PAO1*chpA*(AAA)-FLAG	*chpA*-FLAG with ChpA D2091A, D2092A, and G2093A	This study
PAO1*pilG*-His	*pilG* with a C-terminal His_6 tag at the *pilG* locus	This study
PAO1*pilG*(D58A)-His	*pilG*-His with PilG D58A	This study
PAO1*pilH*-His	*pilH* with a C-terminal His_6 tag at the *pilH* locus	This study
PAO1*pilH*(D52A)-His	*pilH*-His with PilH D52A	This study
PAO1::CTX-P_{pilA}-*lacZ*	PAO1; *pilA* promoter fused to *lacZ* at *attB* site	
PAO1Δ*chpA*::CTX-P_{pilA}-*lacZ*	Δ*chpA*; *pilA* promoter fused to *lacZ* at *attB* site	This study
PAO1Δ*chpA*(comp)::CTX-P_{pilA}-*lacZ*	Δ*chpA*(comp); *pilA* promoter fused to *lacZ* at *attB* site	This study
PAO1Δ*fliC*::CTX-P_{pilA}-*lacZ*	Δ*fliC*; *pilA* promoter fused to *lacZ* at *attB* site	This study
PAO1Δ*fliC*(comp)::CTX-P_{pilA}-*lacZ*	Δ*fliC*(comp); *pilA* promoter fused to *lacZ* at *attB* site	This study
PAO1Δ*pilA*::CTX-P_{pilA}-*lacZ*	Δ*pilA*; *pilA* promoter fused to *lacZ* at *attB* site	This study
PAO1Δ*pilA*(comp)::CTX-P_{pilA}-*lacZ*	Δ*pilA*(comp); *pilA* promoter fused to *lacZ* at *attB* site	This study
PAO1Δ*pilB*::CTX-P_{pilA}-*lacZ*	Δ*pilB*; *pilA* promoter fused to *lacZ* at *attB* site	This study
PAO1Δ*pilA*(comp)::CTX-P_{pilA}-*lacZ*	Δ*pilB*(comp); *pilA* promoter fused to *lacZ* at *attB* site	This study
PAO1Δ*pilG*::CTX-P_{pilA}-*lacZ*	Δ*pilG*; *pilA* promoter fused to *lacZ* at *attB* site	This study
PAO1Δ*pilG*(comp)::CTX-P_{pilA}-*lacZ*	Δ*pilG*(comp); *pilA* promoter fused to *lacZ* at *attB* site	This study
PAO1Δ*pilH*::CTX-P_{pilA}-*lacZ*	Δ*pilH*; *pilA* promoter fused to *lacZ* at *attB* site	This study
PAO1Δ*pilH*(comp)::CTX-P_{pilA}-*lacZ*	Δ*pilH*(comp); *pilA* promoter fused to *lacZ* at *attB* site	This study
PAO1Δ*pilR*::CTX-P_{pilA}-*lacZ*	Δ*pilR*; *pilA* promoter fused to *lacZ* at *attB* site	This study
PAO1Δ*pilR*(comp)::CTX-P_{pilA}-*lacZ*	Δ*pilR*(comp); *pilA* promoter fused to *lacZ* at *attB* site	This study
PAO1$pilT^{\text{Trunc}}$::CTX-P_{pilA}-*lacZ*	*pilT*-Trunc; *pilA* promoter fused to *lacZ* at *attB* site	This study
PAO1Δ*pilT*(comp)::CTX-P_{pilA}-*lacZ*	Δ*pilT*(comp); *pilA* promoter fused to *lacZ* at *attB* site	This study
PAO1Δ*pilU*::CTX-P_{pilA}-*lacZ*	Δ*pilU*; *pilA* promoter fused to *lacZ* at *attB* site	This study
PAO1Δ*pilU*(comp)::CTX-P_{pilA}-*lacZ*	Δ*pilU*(comp); *pilA* promoter fused to *lacZ* at *attB* site	This study
E. coli		
DH5α	*hsdR rec lacZYA* ϕ80 *lacZ*ΔM15	Invitrogen
S17.1λ*pir*	*Thi pro hsdR recA RP4-2*(Tc::Mu)(Km::Tn*7*)	Stratagene
SM10	*thi thr leu tonA lacY supE recA*::*RP4-2*-Tc::Mu Km λ*pir*	15
Plasmids		
pOK12	*E. coli* cloning vector; Km^r	54
pUCPSK	*P. aeruginosa-E. coli* shuttle vector; Ap^r	56
pGEM-T	*E. coli* cloning vector; Ap^r	Promega
pEX100T	Allelic replacement suicide plasmid; Ap^r (Cb^r)	49

Continued on following page

TABLE 1—*Continued*

Strain or plasmid	Genotype and relevant characteristics[a]	Source or reference
pX1918GT	Source of Gm^r cassette; Ap^r	49
mCTX-lacZ	Contains promoterless *lacZ* for constructing transcriptional fusions at the *attB* site; Tc^r	4
mCTX2	Construct for introduction of exogenous DNA fragments at the *attB* site	24
pFLP2	Source of Flp recombinase; Ap^r	23
pAL64	pUCPSK carrying *chpA* with an internal double FLAG tag inserted between the native NotI/NruI sites	39
pEN34	Allelic replacement suicide plasmid; Tc^r	61
pJEN34PAO1KO3	pJEN34 carrying Δ*pilA* on SpeI fragment	This study
pJB4	pOK12 carrying Δ*chpA* on EcoRI/XbaI fragment	61
pJB43	pGEM-T containing 1-kb region 5′ of *pilG*	This study
pJB44	pGEM-T containing 1-kb region 3′ of *pilG*	This study
pJB48	pGEM-T containing 1-kb region 3′ of *pilH*	3
pJB60	XhoI/HindIII fragment from pJB43 and HindIII/XbaI from pJB44 concatamerized and cloned into XhoI/XbaI sites of pOK12	This study
pJB62	pOK12 carrying Δ*pilH* on KpnI/XbaI fragment	3
pJB87	pJEN34 carrying Δ*pilG* on SpeI fragment	This study
pJB96	XhoI/HindIII fragment from pJB43 and HindIII/XbaI from pJB48 concatamerized and cloned into XhoI/XbaI sites of pOK12	This study
pJB97	pJEN34 carrying Δ*pilG*Δ*pilH* on SpeI fragment	This study
pJB100	pEX100T derivative replacing SmaI site with the SpeI site	
pJB109	pJB100 carrying Δ*pilT* on SpeI fragment	This study
pJB110	Gm^r-tagged Δ*pilT* in pJB100; pX1918-derived Gm^r cassette cloned as HindIII fragment into pJB109	This study
pJB111	pJB100 carrying Δ*pilU* on SpeI fragment	This study
pJB112	Gm^r-tagged Δ*pilU* in pJB100; pX1918-derived Gm^r-cassette cloned as HindIII fragment into pJB109	This study
pJB113	pJB100 carrying Δ*pilT* complementation construct on SpeI fragment	This study
pJB114	pJB100 carrying Δ*pilU* complementation construct on SpeI fragment	This study
pJB116	pJB100 carrying Δ*chpA* on SpeI fragment; subcloned from pJB4	This study
pJB118	pJB100 carrying Δ*pilG* on SpeI fragment; subcloned from pJB60	This study
pJB119	pJB100 carrying Δ*pilH* on SpeI fragment; subcloned from pJB62	This study
pJB122	pJB100 carrying Δ*pilB* on SpeI fragment	This study
pJB124	pJB100 carrying *pilH*-His allelic exchange construct on SpeI fragment	This study
pJB126	pJB100 carrying Δ*pilG* complementation construct on SpeI fragment	This study
pJB127	pJB100 carrying *pilG*-His allelic exchange construct on SpeI fragment	This study
pJB163	pJB100 carrying Δ*pilT*Δ*pilU* on the SpeI fragment	This study
pJB202	FLAG-tagged *chpA* histidine kinase domain in pOK12; subcloned as KpnI/ClaI fragment from pAL64	This study
pJB203	pJB100 carrying a *pilT* truncation construct on SpeI fragment	This study
pJB207	*chpA*(AAA) histidine kinase domain in pOK12	This study
pJB212	*pilU* and 1-kb 5′ sequence cloned as SpeI/HindIII fragment into mCTX2	This study
pJB215	pJB100 carrying Δ*fliC* on SpeI fragment	This study
pJB219	Modified pOK12 lacking KpnI and ClaI sites; BglII/SacI fragment removed from pOK12 MCS	This study
pJB220	3′ *chpA* fragment including 1-kb 3′ flanking sequence in pJB219	This study
pJB221	*chpA* including 1 kb of 5′ and 3′ flanking sequence in pJB219	This study
pJB230	pJB100 carrying Δ*fliC* complementation construct on SpeI fragment	This study
pJB231	pJB100 carrying Δ*chpA* complementation construct on SpeI fragment; subcloned from pJB221	This study
pJB232	*chpA*-FLAG, including 1 kb of 5′ and 3′ flanking sequence in pJB219; KpnI/ClaI fragment from pJB202 subcloned into pJB221 from which the corresponding KpnI/ClaI fragment had been removed	This study
pJB233	*chpA*(AAA)-FLAG including 1 kb of 5′ and 3′ flanking sequence in pJB219; KpnI/ClaI fragment from pJB207 subcloned into pJB221 from which the corresponding KpnI/ClaI fragment had been removed	This study
pJB234	pJB100 carrying *chpA*-FLAG allelic exchange on SpeI fragment; subcloned from pJB232	This study
pJB235	pJB100 carrying *chpA*(AAA)-FLAG allelic exchange on SpeI fragment; subcloned from pJB233	This study
pJB241	pJB100 carrying Δ*pilA* complementation construct on SpeI fragment	This study
pJB246	pJB100 carrying Δ*pilB* complementation construct on SpeI fragment	This study
pJB247	pOK12 carrying *pilG*-His allelic-exchange construct on SpeI fragment	This study
pJB248	pOK12 carrying *pilH*-His allelic-exchange construct on SpeI fragment	This study
pJB249	*pilA* reporter construct cloned as XhoI/BamHI fragment into mCTX-*lacZ*	This study
pJB250	pJB100 carrying Δ*pilR* on SpeI fragment	This study
pJB251	pJB100 carrying Δ*pilR* complementation construct on SpeI fragment	This study
pJB252	pOK12 carrying *pilG*(D58A)-His allelic-exchange construct on SpeI fragment	This study
pJB254	pOK12 carrying *pilH*(D582)-His allelic-exchange construct on SpeI fragment	This study
pJB256	pJB100 carrying *pilG*(D58A)-His allelic-exchange construct on SpeI fragment	This study
pJB258	pJB100 carrying *pilH*(D582)-His allelic-exchange construct on SpeI fragment	This study

[a] Cb^r, carbenicillin resistance; Tc^r, tetracycline resistance; Ap^r, ampicillin resistance; Gm^r, gentamicin resistance; Km^r, kanamycin resistance.

To complement the Δ*pilG* mutation, *pilG* and 1 kb of 5′ and 3′ flanking sequence were amplified by using the pilG1(Spe)/pilG4(Spe) PCR primer pair. The product was cloned as a SpeI fragment into pJB100 to form pJB126. pJB126 was transformed into *E. coli* S17.1 and transformants were mated to the Δ*pilG* strain to create a Δ*pilG* derivative complemented for *pilG* at its endogenous locus. The deletion and complementation of *pilH* has been described previously (3).

(v) PilR. 5′ and 3′ *pilR* deletion construct fragments were amplified by using the pilR1/pilR2 and pilR3/pilR4 PCR primer pairs. PCR products were used as templates in an SOE reaction with the pilR1/pilR4 PCR primer pair. The SOE product was cloned as a SpeI fragment into pJB100 for form pJB250. pJB250 was transformed into *E. coli* S17.1, and transformants were mated to PAO1 to create an unmarked Δ*pilR* mutant. This procedure deleted amino acids 4 to 443 of the PilR protein. To complement the Δ*pilR* mutation, *pilR* and 1 kb of 5′ and 3′ flanking sequence were amplified by using the pilR1/pilR4 PCR primer pair. The product was cloned as a SpeI fragment into pJB100 to form pJB251. pJB251 was transformed into *E. coli* S17.1, and transformants were mated to the Δ*pilR* strain to create a Δ*pilR* derivative complemented for *pilR* at its endogenous locus.

TABLE 2. Oligonucleotides used in this study

Primer	Oligonucleotide sequence (5′→3′)[a]
chpA22	GGACTAGTAGATGGCGAGCGAGATGC
chpA25	GAGCTCCTCGCGCAGCGC
chpA26.1	GGCGCGCAACGGCCATTG
chpA29	GGACTAGTCGCAGCGTGCGGCCAGAT
chpA-HisKn-F	CTCCTCACCCTCTCCGCCGCCGCCGCCGGCATCCGCCTC
chpA-HisKn-R	GAGGCGGATGCCGGCGGCGGCGGCGGAGAGGGTGAGGAG
fliC1	GGACTAGTACCGTTTCGTGGTCTCGA
fliC2	TTAGCGCAGCAGAAGCTTAAGGGCCATGGTGATTTCCTCCAAAGG
fliC3	ATGGCCCTTAAGCTTCTGCTGCGCTAAGCCCGGGAACGGTCACTC
fliC4	GGACTAGTATTGATGGCGTCACGCAT
*pilA*1	CCATGGATGCCTAACCTCACCCTTGC
*pilA*1(Spe)	ACTAGTATGCCTAACCTCACCCTTGC
*pilA*2	GAATTCTAAGGTGATCGAAGGTGGCTTGTTTAG
*pilA*3	GAATTCCATGAATATCTCCATTGATATG
*pilA*4	TCTAGATTGATCCGTCCGTCCTGCGG
*pilA*4(Spe)	ACTAGTTTGATCCGTCCGTCCTGCGG
pilA-Reporter-F	CGCGGATCCGAATCTCTCCGTTGATTA
pilA-Reporter-R	CCGCTCGAGGTGTTGGCGGACCAGCTT
pilB1	GCACTAGTATCAACGAGGGCACCCTGCGC
pilB2	TTAATCCTTGGTAAGCTTGTCGTTCATGGGGAAGGAATCGCAGAAGGG
pilB3	ATGAACGACAAGCTTACCAAGGATTAATCCATGGCGGACAAAGCGTTA
pilB4	GCACTAGTTGGATCGCCATGTTGGGAAAG
pilG1	CGGGGTACCCTCAGCGGCTGGGCCACGCCGCG
pilG1(Spe)	GCACTAGTCTCAGCGGCTGGGCCACGCCGCG
pilG2	AAGCTTTTGCTGTTCCATGTTCGCCC
pilG3	AAGCTTAAGGGGCGCATCGTCGGCTC
pilG4	TCTAGAATGAAGGGTTGCAGTGCCGC
pilG4(Spe)	GCACTAGTATGAAGGGTTGCAGTGCCGC
pilG5	TCAGTGGTGGTGGTGGTGGTGGGAAACGGCGTCCACCGGGGT
pilG6	ACCCCGGTGGACGCCGTTTCCCACCACCACCACCACCACTGA
pilG-D58A-F	AACATCATTTTCGTCGCCATCATGATGCCGCGC
pilG-D58A-R	GCGCGGCATCATGATGGCGACGAAAATGATGTT
pilH1	GGTACCCGTTATCGAAGGGCGGGTCC
pilH1(Spe)	GCACTAGTCGTTATCGAAGGGCGGGTCC
pilH4	TCTAGAGCTTTCTCGAAGTCGTTGCG
pilH4(Spe)	GCACTAGTGCTTTCTCGAAGTCGTTGCG
pilH15	TCAGTGGTGGTGGTGGTGGTGGCCCGCCAGCACCGCATTG
pilH16	CAATGCGGTGCTGGCGGGCCACCACCACCACCACCACTGA
pilH-D52A-F	GACGTGGTCCTGATGGCCATCGTCATGCCCGGC
pilH-D52A-R	GCCGGGCATGACGATGGCCATCAGGACCACGTC
pilR1	GGACTAGTCTGCAGCGCATGCGCACC
pilR2	TCAGTCGATGCCAAGCTTTCGGCTCATGCGTGCGGCTTCCGTCAG
pilR3	ATGAGCCGAAAGCTTGGCATCGACTGAAAGTGAAAAGGCCTGTCC
pilR4	GGACTAGTATCGTCTCGCCGCTCTAT
pilT1	GGACTAGTTGGCACACGGCTTTCATGG
pilT1(new)	GGACTAGTAACTCGCCGGCGATCTTC
pilT4	GGACTAGTTGTAGAGCTGGTACAGCGC
pilT5	TCAGAAGTTTTCAAGCTTAATATCCATGGGACTCCCCAATTACAAGC
pilT6	ATGGATATTAAGCTTGAAAACTTCTGATCCTGGCGCCGATCCGC
pilT-Trunc2	CAGGTAATCGAGTCTAGTCTAGACTAGGGGACTCCCCAATTACAAGCAAGCAGG
pilT-Trunc3	GGGAGTCCCCTAGTCTAGACTAGACTCGATTACCTGAACAACACCAAGTACCAC
pilT-Trunc4	GGACTAGTGAAGTTGCACTCATGGTT
*pilU*1	GGACTAGTAACACAAGCAGGTGCATGC
*pilU*4	GGACTAGTAAGGTGAAGAACCAGATCG
*pilU*5	TCAGCGGAAGCGTCTAGAGAATTCCATGATGTTCTCGCTCACTCAGG
*pilU*6	ATGGAATTCTCTAGACGCTTCCGCTGAACCGTCTTCAGTAGGCCAGC
pilT*pilU*1	TCAGCGGAAGCGAATATCCATGGGACTCCCCAATTACAAGC
pilT*pilU*2	ATGGATATTCGCTTCCGCTGAACCGTCTTCAGTAGGCCAGC
pilU-CTX-Spe-F	GGACTAGTGACCGGGTGGTCGACGTGTTC
pilU-CTX-Hind-R	CCCAAGCTTTCAGCGGAAGCGCCGGCCGGC

[a] Restriction endonuclease sequences are underlined.

(vi) PilT. 5′ and 3′ *pilT* deletion construct fragments were amplified by using the pilT1/pilT5 and pilT6/pilT4 PCR primer pairs. PCR products were used as templates in an SOE reaction with the pilT1/pilT4 PCR primer pair. The SOE product was cloned as a SpeI fragment into pJB100 for form pJB109. pJB109 was transformed into *E. coli* S17.1, and transformants were mated to PAO1 to create an unmarked Δ*pilT* mutant. This procedure deleted amino acids 4 to 342 of the PilT protein. To complement the Δ*pilT* mutation, *pilT* and 1 kb of 5′ and 3′ flanking sequence were amplified by using the pilT1/pilT4 PCR primer pair. The product was cloned as a SpeI fragment into pJB100 to form pJB113. pJB113 was transformed into *E. coli* S17.1, and transformants were mated to the Δ*pilT* mutant to create a Δ*pilT* derivative complemented for *pilT* at its endogenous locus.

The *pilT* truncation mutation (*pilT*^{Trunc}) deletes 429 bp of the *pilT* coding sequence including the start codon (amino acids 1 to 143 of the PilT protein) and introduces stop codons in all three reading frames. The mutant retains 783 bp of sequence upstream of *pilU*. The 5′ and 3′ truncation construct fragments were amplified by using the pilT1(new)/pilT-Trunc2 PilT-Trunc3/pilT-Trunc4 PCR primer pairs. PCR products were used as templates in an SOE reaction with the pilT1(new)/pilT-Trunc4 PCR primer pair. The SOE product was cloned as a SpeI fragment into pJB100 for form pJB203. pJB203 was transformed into *E. coli* S17.1, and transformants were mated to PAO1 to create the *pilT*^{Trunc} mutant.

(vii) PilU. 5′ and 3′ *pilU* deletion construct fragments were amplified by using the *pilU*1/*pilU*5 and *pilU*6/*pilU*4 PCR primer pairs. PCR products were used as templates in an SOE reaction with the *pilU*1/*pilU*4 PCR primer pair. The SOE product was cloned as a SpeI fragment into pJB100 for form pJB111. pJB111 was transformed into *E. coli* S17.1, and transformants were mated to PAO1 to create an unmarked Δ*pilU* mutant. This procedure deleted amino acids 4 to 380 of the PilU protein. To complement Δ*pilU*, *pilU* and 1 kb of 5′- and 3′-flanking sequence were amplified by using the *pilU*1/*pilU*4 PCR primer pair. The product was cloned as a SpeI fragment into pJB100 to form pJB114. pJB114 was transformed into *E. coli* S17.1, and transformants were mated to the Δ*pilU* mutant to create a Δ*pilU* derivative complemented for *pilU* at its endogenous locus.

(viii) FliC. 5′ and 3′ *fliC* deletion construct fragments were amplified by using the fliC1/fliC4 and fliC3/fliC4 PCR primer pairs. PCR products were used as templates in an SOE reaction with the fliC1/fliC4 PCR primer pair. The SOE product was cloned as a SpeI fragment into pJB100 for form pJB215. pJB215 was transformed into *E. coli* S17.1, and transformants were mated to PAO1 to create an unmarked Δ*fliC* mutant. This procedure deleted amino acids 4 to 486 of the FliC protein. To complement the Δ*fliC* mutation, *fliC* and 1 kb of 5′- and 3′-flanking sequence were amplified by using the flic1/flic4 PCR primer pair. The product was cloned as a SpeI fragment into pJB100 to form pJB230. pJB230 was transformed into *E. coli* S17.1, and transformants were mated to the Δ*fliC* mutant to create a Δ*fliC* derivative complemented for *fliC* at its endogenous locus.

A pEX100T-based *chpA* deletion construct was made by subcloning the *chpA* deletion construct as a SpeI fragment from pJB4 to pJB100 to form pJB116. pJB116 was transformed into *E. coli* S17.1, and transformants were mated to PAO1Δ*pilH*, PAO1Δ*pilT*, PAO1Δ*pilU*, and PAO1Δ*pilT*Δ*pilU* constructs (see below) to create PAO1Δ*chpA*Δ*pilH*, PAO1Δ*chpA*Δ*pilT*, PAO1Δ*chpA*Δ*pilU*, and PAO1Δ*chpA*Δ*pilT*Δ*pilU*, respectively.

To construct PAO1Δ*pilG*Δ*pilH*, the 5′ deletion construct from pJB43 was excised as an XhoI/HindIII fragment, concatamerized with the 3′ deletion construct from pJB48 excised as a HindIII/XbaI fragment, and cloned as an XhoI/XbaI fragment into pOK12 to form pJB96. The deletion construct was excised from pJB96 as a SpeI fragment and ligated into the allelic exchange vector pJEN34 to form pJB97. pJB97 was transformed into *E. coli* S17.1, and transformants were mated to PAO1 to create an unmarked Δ*pilG* Δ*pilH* mutant. Gentamicin-resistant derivatives of the *pilT* and *pilU* deletion constructs were made by subcloning a gentamicin resistance encoding cassette as a HindIII fragment from pX1918GT (46) into pJB109 and pJB111 to form pJB110 and pJB112, respectively. pJB110 and pJB112 were transformed into *E. coli* S17.1, and transformants were mated to PAO1Δ*pilG* to created PAO1Δ*pilG*Δ*pilT*-gent and PAO1Δ*pilG*Δ*pilU*-gent. PAO1Δ*pilG*Δ*pilT*-gent and PAO1Δ*pilGpilU*-gent were then mated to S17.1 strains carrying pJB109 and pJB111 to create the PAO1Δ*pilG*Δ*pilT* and PAO1Δ*pilG*Δ*pilU* constructs. A pEX100T-based *pilG* deletion construct was made by subcloning the *pilG* deletion construct as a SpeI fragment from pJB59 to pJB100 to form pJB118. pJB118 was transformed into *E. coli* S17.1, and transformants were mated to the Δ*pilT* Δ*pilU* strain (see below) to create strain PAO1Δ*pilG*Δ*pilT*Δ*pilU*.

Strains PAO1Δ*pilB*Δ*pilH* and PAO1Δ*pilB*Δ*pilT*Δ*pilU* were constructed by mating the Δ*pilH* and Δ*pilT* Δ*pilU* strains respectively, to *E. coli* S17.1 carrying pJB122. The PAO1Δ*pilB*Δ*pilT* and PAO1Δ*pilB*Δ*pilU* strains were constructed by mating the PAO1Δ*pilB* strain to *E. coli* S17.1 carrying pJB109 and pJB111, respectively.

5′ and 3′ PAO1Δ*pilT*Δ*pilU* deletion construct fragments were amplified by using the pilT1/pilT*pilU*1 and pilT*pilU*2/*pilU*4 PCR primer pairs. PCR products were used as templates in an SOE reaction with the pilT1/*pilU*4 PCR primer pair. The SOE product was cloned as a SpeI fragment into pJB100 for form pJB163. pJB163 was transformed into *E. coli* S17.1 and transformants were mated to PAO1 to create PAO1Δ*pilT*Δ*pilU*. A pEX100T-based *pilH* deletion construct was made by subcloning the *pilH* deletion construct as a SpeI fragment from pJB62 to pJB100 to form pJB119. pJB119 was transformed into *E. coli* S17.1, and transformants were mated to Δ*pilT*, Δ*pilU*, and Δ*pilT* Δ*pilU* constructs to create strains PAO1Δ*pilH*Δ*pilT*, PAO1Δ*pilH*Δ*pilU*, and PAO1Δ*pilH*Δ*pilT*Δ*pilU*, respectively.

(ix) PAO1Δ*pilT*$^{CTX\text{-}pilU}$ strains. *pilU*, along with 1,000 bp of upstream sequence, was introduced in single copy onto the *P. aeruginosa* chromosome at the phage attachment site *attB* by using the mini-CTX system (22). The CTX-*pilU* construct was amplified by using the *pilU*-CTX-Spe-F(1kb)/*pilU*-CTX-Hind-R PCR primer pair. The PCR product was cloned as a SpeI/HindIII fragment into mini-CTX2 to form pJB212. pJB212 was transformed into *E. coli* S17.1, and transformants were mated to all *pilT* mutant strains except the PAO1Δ*pilT*^{Trunc} and PAO1Δ*pilT*Δ*pilU* strains to create PAO1Δ*pilT*$^{CTX\text{-}pilU}$ derivatives. The plasmid backbone was removed by mating strains to *E. coli* SM10 carrying pFLP2, as described previously (22).

(x) *chpA*-FLAG and *chpA* point mutants. The region of *chpA* encoding the histidine kinase domain and the 2X-FLAG tag was subcloned as a ClaI/KpnI fragment from pAL64 (37) into pOK12 to form pJB202. The KpnI/ClaI fragment was subcloned from pJB202 into pJB221 from which the corresponding ClaI/KpnI fragment had been removed to form pJB232. Full-length *chpA*-FLAG, including 1 kb 5′ and 3′ flanking sequence, was subcloned into pJB100 to form pJB234. pJB234 was transformed into *E. coli* S17.1, and transformants were mated to the Δ*chpA* mutant to create PAO1Δ*chpA*-FLAG.

pJB202 was the substrate for a QuickChange (Stratagene) mutagenesis reaction using the chpA-HisKn-F/chpA-HisKn-R PCR primer pair. The mutation replaces each of the three residues in the signature DXG motif of the G1 box of ChpA with alanines (D2091A, D2092A, and G2093A), *chpA*(AAA)-FLAG. The mutated histidine kinase domain, including the 2X-FLAG tag, was subcloned as a KpnI/ClaI fragment from pJB207 into pJB221 from which the corresponding ClaI/KpnI fragment had been removed to form pJB233. Full-length *chpA*(AAA)-FLAG, including 1 kb of 5′ and 3′ flanking sequence, was subcloned into pJB100 to form pJB235. pJB235 was transformed into *E. coli* S17.1, and transformants were mated to the Δ*chpA* mutant to create PAO1Δ*chpA*(AAA)-FLAG.

(xi) *pilG*-His, *pilH*-His, and *pilG* and *pilH* point mutants. 5′ and 3′ allelic-exchange constructs to generate C-terminal His_6-tagged derivatives of the *pilG* and *pilH* mutants were amplified by using the pilG1(Spe)/pilG5 and pilG6/pilG4(Spe) and the pilH1/pilH15 and pilH16/pilH4 PCR primer pairs, respectively. PCR products were used as templates in SOE reactions with the pilG1(Spe)/pilG4(Spe) and pilH1/pilH4 primer pairs. The SOE products were cloned blunt into SmaI-digested pEX100T to form pJB124 (*pilH*-His) and pJB127 (*pilG*-His). pJB124 and pJB127 were transformed into *E. coli* S17.1, and transformants were mated to Δ*pilH* and Δ*pilG* mutants to create the *pilH*-His and *pilG*-His constructs, respectively.

pilG-His and *pilH*-His allelic-exchange constructs were amplified from pJB127 and pJB124, respectively, by using pilG1(Spe)/pilG4(Spe) and pilH1(Spe)/pilH4(Spe) PCR primer pairs cloned as Spe fragments into pOK12 to form pJB247 and pJB248. pJB247 and pJB248 were substrates for QuickChange (Stratagene) mutagenesis reactions by using pilG-D58A-F/pilG-D58A-R and pilH-D52A-F/pilH-D52A-R PCR primer pairs to form pJB252 and pJB254, respectively. The *pilG*(D58A)-His and *pilH*(D52A)-His allelic-exchange constructs were subcloned as SpeI fragments from pJB252 and pJB254 into pJB100 to form pJB256 and pJB258. pJB256 and pJB258 were transformed into *E. coli* S17.1 and transformants were mated to Δ*pilG* and Δ*pilH* strains to create PAO1Δ*pilG*(D58A)-His and PAO1Δ*pilH*(D52A)-His.

P_{pilA}-*lacZ* reporter strains. A transcriptional fusion of the *pilA* promoter to *lacZ* was introduced in single copy onto the *P. aeruginosa* chromosome at the phage attachment site *attB* using the mini-CTX system (4). A 500-bp portion of sequence upstream of the *pilA* start codon was amplified by using the pilA-Reporter-F/pilA-Reporter-R PCR primer pair. The PCR product was cloned as an XhoI/BamHI fragment into mCTX2-*lacZ* to form pJB249. pJB249 was transformed into *E. coli* S17.1, and transformants were mated to all single mutant strains (except the Δ*pilT* strain) and *pilT*^{Trunc} to create CTX-P_{pilA} derivatives. The plasmid backbone was removed by mating strains to *E. coli* SM10 carrying pFLP2, as described previously (4).

TM assay. Subsurface twitching motility (TM) stab assays were performed as previously described (1). TM was quantified by taking three separate measurements of twitching zone diameter from five independent stabs.

Generation of the α-PilA antibody. Polyclonal α-PilA antibodies were raised commercially in rabbits against the synthetic peptide WACKSTQDPMFTP KGCD (Invitrogen). The peptide represents amino acids 132 to 148 of PilA. For the present study, serum collected 8 weeks postinoculation with the antigen was used.

Immunoblotting. Isolation of intracellular pilin for cells cultured on solid media was performed as follows. A portion (100 μl) of a 2-ml LB culture grown shaking overnight at 37°C was plated onto 1.5% LB agar and grown at 37°C for 16 h. After growth, bacteria were scraped from the agar surface and resuspended in 5 ml of phosphate-buffered saline (PBS). A volume of cells equivalent to an optical density at 600 nm (OD_{600}) of 5.0 was brought up to 1 ml in PBS. Cells

were vortexed for 30 min to remove surface pili and harvested by centrifugation (20,000 × *g* for 10 min). The supernatant was removed, and cells were resuspended in 100 μl of BugBuster protein extraction reagent (Novagen). Then, 1 μl of Benzonase nuclease (Novagen) was added, and the resuspended cells were incubated by gentle mixing at room temperature for 30 min. Cellular debris was removed by centrifugation (20,000 × *g* for 10 min), and 90 μl of supernatant was added to 90 μl of 2× NuPage LDS protein sample buffer (Invitrogen) and 20 μl of 10× NuPage sample reducing agent (Invitrogen). Samples were boiled for 5 min. Protein concentration was determined by using a Bio-Rad protein assay. To isolate surface pili, bacteria were grown as described above at 37°C for 16 h on 1.5% LB agar, scraped from the agar surface, and resuspended in 5 ml of PBS. A volume of cells equivalent to an OD_{600} of 20.0 was brought up to 1 ml in PBS. Cells were vortexed at room temperature for 30 min to remove surface pili. The suspension was centrifuged at room temperature (20,000 × *g* for 10 min), and the supernatant was collected and centrifuged a second time (20,000 × *g* for 10 min) to remove all cellular debris. The resulting supernatant was incubated overnight at 4°C in 100 mM $MgCl_2$ to precipitate pili, as described previously (1). The precipitate was collected by centrifugation at 4°C (20,000 × *g* for 20 min), the supernatant was removed, and the pellet was resuspended in 100 μl of PBS and 100 μl of 2× NuPage LDS protein sample buffer (Invitrogen), including 1× NuPage sample reducing agent (Invitrogen). The samples were boiled for 5 min.

Isolation of intracellular pilin for cells cultured in liquid medium was performed as follows. Bacteria were grown shaking at 37°C for 16 h in 10 ml of LB medium. A volume of cells equivalent to an OD_{600} of 5.0 was brought up to 1.5 ml in PBS and processed as described above. To isolate surface pili, bacteria were grown shaking at 37°C for 16 h in 10 ml of LB broth. A volume of cells equivalent to an OD_{600} of 20.0 was brought up to 6 ml in PBS. Cells were harvested by centrifugation (6,000 × g for 10 min), resuspended in 1 ml of PBS and processed as described above.

To detect cell-associated and surface pilin for cells cultured on both solid medium and in liquid medium, 15 μg of total cell-associated protein or 10 μl of surface pilin samples (1/20 of the total sample) was separated on Novex-NuPAGE 12% Bis-Tris SDS-PAGE gels (Invitrogen) and electroblotted onto Immun-Blot PVDF membrane (Bio-Rad) in a previously described Tris-glycine system (50). Membranes were blocked in 5% skim milk and probed with a 1:100,000 dilution of primary α-PilA antibody in 5% skim milk powder (0.05% Tween 20) in PBS. Membranes were then incubated with a 1:25,000 dilution of goat anti-rabbit immunoglobulin G conjugated with horseradish peroxidase (Jackson Immunoresearch Laboratories) in 5% skim milk powder (0.05% Tween 20) in PBS, followed by detection by enhanced chemiluminescence using the Amersham ECL Western blotting detection kit (GE Healthcare).

Cell-associated and surface flagellin samples for both plate and broth cultured cells were prepared as described for pilin samples. Detection of cell-associated and surface flagellin for both plate- and broth-cultured cells was carried out as described for pilin immunoblots, with the exception that membranes were probed with a 1:200,000 dilution of anti-FlaB antibody (kindly provided by Daniel Wozniak, Ohio State University [18]).

To quantify the levels of surface pili, samples were run in triplicate and immunoblotted for PilA and FliC as described above. Images of immunoblots were acquired on the ChemiDoc XRS (Bio-Rad) and quantified by using Quantity-One image analysis software. Surface pili levels were normalized to FliC. Isolation and detection of PAO1Δ*chpA*-FLAG and PAO1Δ*chpA*(AAA)-FLAG was performed as described previously (37). Briefly, to prepare protein samples, cells were harvested from 2 ml of culture grown shaking for 16 h at 37°C, resuspended in 400 μl of SDS-PAGE sample buffer, passaged through a 27.5 gauge needle three times, and boiled for 5 min. Then, 40 μl (1/10 of total sample volumes) was separated by SDS-PAGE and immunoblotted with 2.5 μg of α-FLAG M2 monoclonal antibody/ml using 2.5 μg of α-FLAG M2 monoclonal antibody (Sigma)/ml.

Phage sensitivity assays. Phage sensitivity was assayed using the Tfp-specific *P. aeruginosa* bacteriophage PO4 (kindly provided by Lori Burrows, McMaster University), as previously described (52). Briefly, the phage stock was titered by adding 10 μl of serial diluted phage to 100 μl of stationary-phase PAO1, followed by incubation at room temperature for 30 min, and then added to 3 ml of 0.8% LB top agar, poured onto 1.5% LB agar, and incubated overnight at 37°C. To determine the phage sensitivity of mutant strains, triplicate cultures started from single colonies were grown shaking for 16 h at 37°C. Next, 100 μl of culture was infected with 10 μl of diluted phage, followed by incubation at room temperature for 30 min. After incubation, samples were added to 3 ml of 0.8% LB top agar, followed by incubation for 16 h at 37°C. To quantify the data, the plaques were counted, and the PFU of phage/ml were determined.

β-Galactosidase assays. β-Galactosidase assays were performed as previously described (52) with the following modifications. For assays performed on strains cultured in liquid media, cultures started from single colonies were grown in triplicate with shaking for 16 h at 37°C in 5 ml of LB medium. For assays performed on strains cultured on solid media, cultures started from single colonies were grown in triplicate shaking overnight at 37°C in 2 ml of LB medium. Then, 100 μl of overnight culture was plated to 1.5% LB agar and grown for 16 h. After growth, cells were scraped from the agar surface, and resuspended in 5 ml of PBS and diluted to an OD_{600} of 4.0 before being assayed as described previously (52). Optical densities (OD_{600} and OD_{420}) were recorded by using a SPECTRAmax microplate spectrophotometer (Molecular devices) and SoftMaxPro 4.3.1. Specific activities were calculated relative to the OD_{600}.

Statistical analysis. Statistical significance was determined by analysis of variance using Instat software. Differences were considered to be significant at a P of <0.05.

RESULTS

***chpA*, *pilG*, and *pilB* regulate pilus extension.** We constructed in-frame *chpA* (55), *pilG*, *pilH* (3), *pilB*, *pilT*, and *pilU* deletion mutants in strain PAO1 and assayed them for Tfp function, including TM, intracellular and surface pilin levels, and phage sensitivity. The present study represents the first in-depth phenotypic analysis of in-frame deletions of these genes in the same strain background and is the first instance in which all mutations have been complemented by reintroduction of the genes onto the chromosome at their endogenous loci. TM was measured by the subsurface stab assay. To determine surface and intracellular pilin levels, plate-grown bacteria were harvested after 16 h. Surface pili were sheared by vigorous vortexing, the bacteria were removed by centrifugation, and the sheared pili were precipitated from the supernatant. Pilin in the pelleted bacteria constituted the intracellular pilin fraction. Infection with phage PO4, which requires Tfp for adsorption, is a sensitive measure of surface pili. For example, some mutants which lack surface pili by Western analysis remain sensitive to infection by phage PO4 (56).

Consistent with previous results (12, 13, 42, 54–56), all mutants had defects in TM (Fig. 2A and B and Fig. 3A and B). As expected (42), the Δ*pilB* mutant lacked surface pili (Fig. 2C) and was resistant to infection with phage PO4 (Table 3). The Δ*pilG* mutant also lacked detectable surface pili, and the Δ*chpA* mutant had greatly reduced surface pili as determined by Western blot analysis (Fig. 2C). Both mutants, however, remained susceptible to phage infection (Table 3), suggesting that they assembled small amounts of functional surface pili. With the exception of *pilB* and *pilT* single, double, and triple mutants, infection of all strains with phage PO4 produced nearly as many plaques as when wild-type (WT) PAO1 was infected. However, in all cases plaques formed on mutant lawns were turbid compared to plaques formed on WT lawns (data not shown). All mutants had wild-type levels of flagellin on the cell surface, indicating that presentation of surface structures other than Tfp is not affected in these mutant backgrounds (Fig. 2C). Although Western blot analysis of cell lysates showed a slight decrease in pilin production in the Δ*pilB*, Δ*pilG*, and Δ*chpA* mutants compared to the wild type (Fig. 2C), this decrease is not sufficient to account for their profound defect in TM and surface presentation. TM, pilin production, surface piliation, and phage sensitivity could be complemented by reintroduction of each of the genes at their endogenous chromosomal loci (Fig. 2). Taken together, and consistent with previous observations, these data suggest that *chpA*, *pilG*, and *pilB* are involved in the regulation of pilus extension.

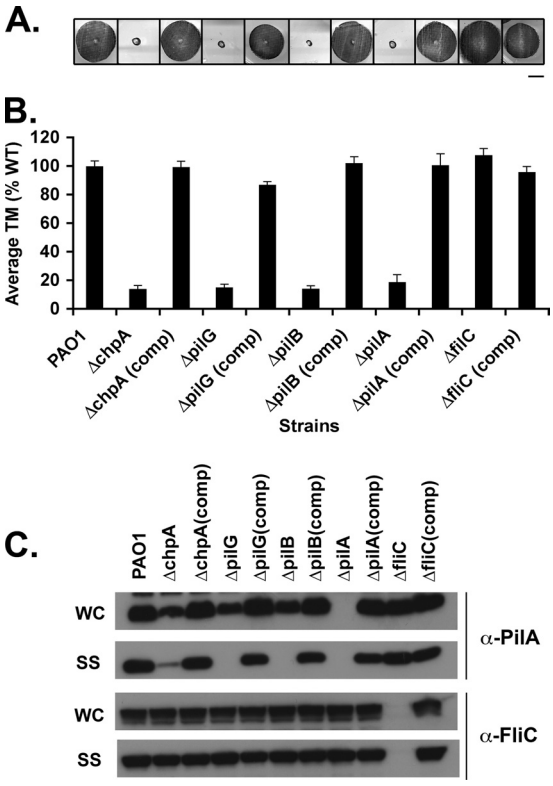

FIG. 2. Assays of pilus function for mutants defective in pilus extension. (A) Subsurface TM assay of PAO1, the indicated in-frame deletion mutants, and complemented (comp) strains in which the wild-type gene was reintroduced at its endogenous locus. TM assays were performed by the subsurface stab method, followed by Coomassie blue staining, as described previously (1). Bar, 1 cm. (B) Graph depicting TM zone diameters for the indicated strains. The diameter is expressed as a percentage of PAO1 TM. Shown are the means ± the standard deviation (SD, $n = 5$). The residual zones observed in Δ*pilA*, Δ*chpA*, Δ*pilG*, and Δ*pilB* strains represent colony growth. (C) Intracellular and surface pilin and flagellin levels. For the indicated strains, surface structures (SS) including pili and flagella were sheared by vigorous vortexing of bacteria cultured on solid media and separated from cells (WC) by centrifugation. The sheared pili and flagella were precipitated. WC (15 μg of total protein) and SS (5% of the total resuspended volume of the precipitate) samples were separated by SDS-PAGE and immunoblotted with a polyclonal antibody to PilA (α-pilA) or to FliC (α-FliC).

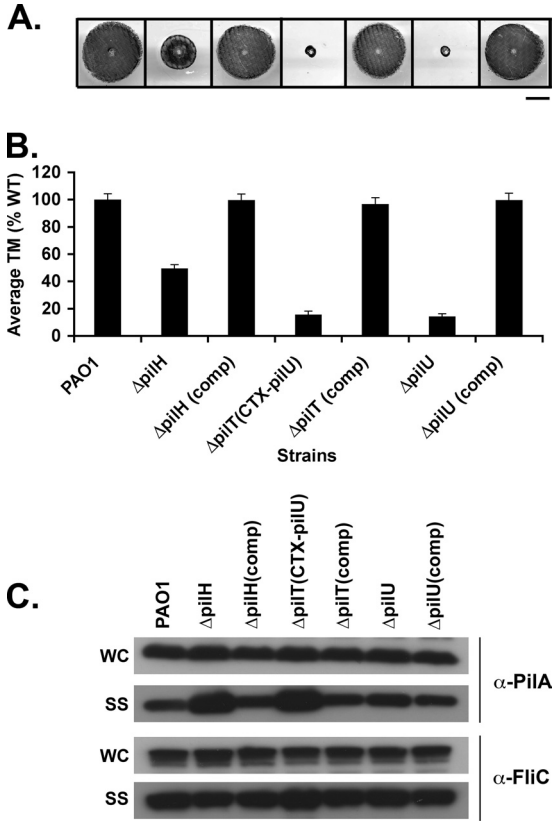

FIG. 3. Assays of pilus function for mutants defective in pilus retraction. (A) Subsurface TM assays were performed as described in Fig. 1. The bar represents 1 cm. (B) Graph depicting average twitching zone diameters for the indicated strains. Shown are the means ± the SD ($n = 5$) The residual zone observed in the Δ*pilT* and Δ*pilB* strains represents colony growth and is similar to that of the Δ*pilA* strain. (C) Surface structures (SS) and intracellular (WC) preparations of the indicated strains were immunoblotted with a polyclonal antibody to PilA (α-pilA) or to FliC (α-FliC), as described in Fig. 2.

***pilH* and *pilT* regulate pilus retraction.** We next examined Δ*pilH*, Δ*pilT*, and Δ*pilU* mutants to confirm their role in the regulation of pilus retraction. All three of these mutants, in contrast to the Δ*chpA*, Δ*pilG*, and Δ*pilB* mutants, had WT levels of intracellular pilin (Fig. 3C). The Δ*pilT* mutant was completely defective for TM, having TM zones comparable to those of a Δ*pilA* mutant (Fig. 3A and B). It had significantly increased levels of surface pili relative to WT ($P < 0.05$, Fig. 5D) and was resistant to phage PO4 (Table 3). The Δ*pilU* mutant showed greatly decreased TM (Fig. 3A and B) but was phage sensitive (Table 3) and had levels of surface pili statistically indistinguishable from the WT (Fig. 3C and 5D). The Δ*pilH* mutant had a TM zone intermediate to wild type and Δ*pilA* (Fig. 3A and B) and exhibited increased levels of surface pili relative to the WT ($P < 0.05$, Fig. 3C and 5D) but, in contrast to the Δ*pilT* mutant, it was phage PO4 sensitive (Table 3). The morphology of plaques formed by PO4 phage on the Δ*pilH* mutant was distinguished by a tear-drop-shaped zone of lysis and poorly defined plaques, even at low titers of phage (data not shown). This phenotype is unique among the Tfp regulatory factors addressed in the current study and does not appear to have been described for any other factor involved in the biogenesis or function of Tfp. For each of these strains, WT TM, surface piliation, and phage sensitivity could be restored by reintroduction of each of the genes at their endogenous chromosomal loci (Fig. 3).

Whereas all of the other mutants (i.e., the Δ*chpA*, Δ*pilG*, Δ*pilB*, Δ*pilH*, and Δ*pilU* mutants) could be complemented for TM in *trans*, the Δ*pilT* mutant could only be complemented by the reintroduction of *pilT* onto the chromosome at the *pilT* locus (data not shown). This finding suggests that the in-frame deletion of *pilT* might affect transcription of the adjacent *pilU* gene by disrupting *cis*-regulatory sequences required for *pilU* transcription located within the *pilT* coding sequence. Indeed, previous studies suggest that *pilT* and *pilU* are transcribed separately (56). We constructed a derivative of the Δ*pilT* mutant (PAO1Δ$pilT^{CTX\text{-}pilU}$) in which the *pilU* gene, including 1,000 bp of upstream sequence, was introduced at an exoge-

TABLE 3. Sensitivity of various strains to infection by the pilus-specific phage PO4

Strain	Strain sensitivity (avg PFU/ml ± SD [10^9])[a]
PAO1	3.96 ± 0.53
PAO1Δ*chpA*	3.30 ± 0.70
PAO1Δ*chpA*(comp)	3.75 ± 0.79
PAO1Δ*pilG*	2.85 ± 0.72
PAO1Δ*pilG*(comp)	4.52 ± 0.66
PAO1Δ*pilB*	0.00 ± 0.00*
PAO1Δ*pilB*(comp)	3.92 ± 0.32
PAO1Δ*pilA*	0.00 ± 0.00*
PAO1Δ*pilA*(comp)	4.12 ± 0.56
PAO1Δ*fliC*	3.92 ± 0.56
PAO1Δ*fliC*(comp)	5.41 ± 0.14
PAO1Δ*pilH*	2.96 ± 0.58†
PAO1Δ*pilH*(comp)	3.48 ± 0.45
PAO1Δ$pilT^{CTX\text{-}pilU}$	0.00 ± 0.00*
PAO1Δ*pilT*(comp)	3.39 ± 0.17
PAO1Δ*pilU*	2.88 ± 0.33
PAO1Δ*pilU*(comp)	4.11 ± 0.48
PAO1Δ*chpA*Δ*pilH*	4.00 ± 0.45†
PAO1Δ*chpA*Δ$pilT^{CTX\text{-}pilU}$	0.00 ± 0.00*
PAO1Δ*chpA*Δ*pilU*	1.85 ± 0.30
PAO1Δ*chpA*Δ*pilT*Δ*pilU*	0.00 ± 0.00*
PAO1Δ*pilG*Δ*pilH*	3.93 ± 0.72†
PAO1Δ*pilG*Δ$pilT^{CTX\text{-}pilU}$	0.00 ± 0.00*
PAO1Δ*pilG*Δ*pilU*	3.07 ± 0.78
PAO1Δ*pilG*Δ*pilT*Δ*pilU*	0.00 ± 0.00*
PAO1Δ*pilB*Δ*pilH*	0.00 ± 0.00*
PAO1Δ*pilB*Δ$pilT^{CTX\text{-}pilU}$	0.00 ± 0.00*
PAO1Δ*pilB*Δ*pilU*	0.00 ± 0.00*
PAO1Δ*pilB*Δ*pilT*Δ*pilU*	0.00 ± 0.00*
PAO1Δ*pilH*Δ$pilT^{CTX\text{-}pilU}$	0.00 ± 0.00*
PAO1Δ*pilT*Δ*pilU*	0.00 ± 0.00*
PAO1Δ*pilH*Δ*pilU*	2.87 ± 0.83†
PAO1Δ*pilH*Δ*pilT*Δ*pilU*	0.00 ± 0.00*
PAO1*chpA*-FLAG	3.45 ± 0.63
PAO1Δ*chpA*(AAA)-FLAG	3.28 ± 0.63
PAO1*pilG*-His	3.17 ± 0.29
PAO1*pilG*(D58A)-His	2.99 ± 0.39
PAO1*pilH*-His	3.31 ± 0.34
PAO1*pilH*(D52A)-His	4.23 ± 0.23†

[a] *, No plaques were detectable even when strains were infected with 10^9 phage. †, The Δ*pilH* plaque morphology was distinguished by large zones of seemingly directional lysis and poorly defined plaques.

nous chromosomal locus using the mini-CTX system (22). This mutant was TM defective, had increased levels of surface pili, was phage resistant, and had WT levels of intracellular pilin and could be complemented for TM by expression of *pilT* in *cis* or in *trans* (Fig. 3, Table 3, and data not shown). This strain was used in the remainder of our studies except where indicated.

The phenotype of Δ*pilT* mutants differed from that of Δ*pilH* mutants in several important ways. PAO1Δ$pilT^{CTX\text{-}pilU}$ had increased surface pili relative to the Δ*pilH* mutant by Western blot analysis (Fig. 3C and 5C), although the difference was not statistically significant (Fig. 5D). PAO1Δ$pilT^{CTX\text{-}pilU}$ was phage PO4 resistant, whereas the Δ*pilH* mutant was phage PO4 sensitive. Together, these data are consistent with the idea that PilT functions as a motor protein which serves to drive pilus retraction and whose activity is enhanced but is not completely dependent upon PilH.

***chpA*, *pilG*, and *pilB* function upstream of *pilH*, *pilT*, and *pilU*.** We hypothesize that ChpA acts as a histidine kinase to phosphorylate PilG and/or PilH. Phosphorylated PilG, in turn modulates PilB-dependent pilus extension, while phosphorylated PilH is required for PilT- and/or PilU-dependent pilus retraction. This model leads to the testable genetic prediction that double mutants in any factor involved in regulating pilus extension (*chpA*, *pilG*, or *pilB*) and any factor involved in regulating pilus retraction (*pilH*, *pilT*, and *pilU*) should have reduced surface pili. We constructed informative double mutants and assayed them for TM, intracellular and surface pilin levels, and phage sensitivity. All double mutants were defective for TM (Fig. 4A and B). This finding is most notable in the case of *pilH* double mutants, which no longer exhibit any TM, indicating that ChpA, PilG, and PilB all function upstream of PilH.

chpA double mutants (PAO1Δ*chpA*Δ*pilH*, PAO1Δ*chpA*Δ$pilT^{CTX\text{-}pilU}$, and PAO1Δ*chpA*Δ*pilU*) retained some surface piliation (Fig. 4C), although less than seen in the single *pilH*, *pilT*, or *pilU* mutants (Fig. 3C) but more than seen in the single *chpA* mutant (Fig. 2C). Furthermore, PAO1Δ*chpA*Δ*pilH* and PAO1Δ*chpA*Δ$pilT^{CTX\text{-}pilU}$ exhibited phage sensitivity similar to PAO1Δ*pilH* and PAO1Δ$pilT^{CTX\text{-}pilU}$ (Table 3), respectively,

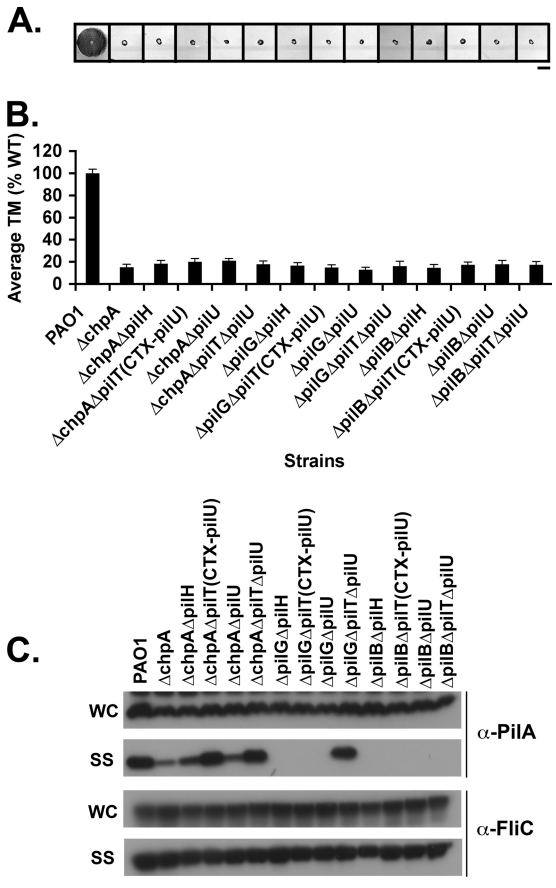

FIG. 4. *chpA*, *pilG*, and *pilB* function upstream of *pilH*, *pilT*, and *pilU*. (A) Subsurface TM assays were performed as described in Fig. 1. Bar, 1 cm. (B) Graph depicting average TM zone diameters for the indicated strains. Shown are the means ± the SD ($n = 5$). The residual zone of TM in all of the mutants represents colony growth and is similar to of the Δ*pilA* mutant. (C) Surface structures (SS) and intracellular (WC) preparations of the indicated strains were immunoblotted with a polyclonal antibody to PilA (α-pilA) or to FliC (α-FliC), as described in Fig. 2.

indicating that PilH and PilT function downstream of ChpA. The observation that PAO1Δ*chpA*Δ*pilU* shows reduced surface piliation relative to WT (Fig. 4C), where the Δ*pilU* mutant has surface pilin levels similar to WT (Fig. 3C) indicates that, whatever role PilU plays in the regulation of pilus dynamics, it functions downstream of ChpA. Thus, we conclude that ChpA functions upstream of PilH, PilT, and PilU.

We next compared various combinations of *pilG* or *pilB* double mutants. PAO1Δ*pilG*Δ*pilH* and PAO1Δ*pilG*Δ*pilT*$^{\text{CTX-}pilU}$ had the same phage sensitivity as PAO1Δ*pilH* and PAO1 Δ*pilT*$^{\text{CTX-}pilU}$, respectively (Table 3). Likewise, PAO1Δ*pilB* Δ*pilH* and PAO1Δ*pilB*Δ*pilU* were resistant to phage infection. PAO1Δ*pilG*Δ*pilH*, PAO1Δ*pilG*Δ*pilT*$^{\text{CTX-}pilU}$, PAO1Δ*pilG*Δ*pilU*, PAO1Δ*pilB*Δ*pilH*, PAO1Δ*pilB*Δ*pilT*$^{\text{CTX-}pilU}$, and PAO1*pilB* Δ*pilU* all lacked surface pili (Fig. 4C). These data are consistent with the model that both PilG and PilB function upstream of PilH, PilT, and PilU.

Our work (Table 3) and others (3, 12) have shown that *chpA* and *pilG* mutants remain susceptible to infection by phage PO4, whereas *pilB* mutants are immune to this pilus-specific phage (42). These observations suggest that some PilB-dependent pilus extension must occur in the absence of upstream signaling input from either ChpA or PilG. To test this hypothesis, we constructed PAO1Δ*chpA*Δ*pilT*Δ*pilU*, PAO1Δ*pilG*Δ*pilT* Δ*pilU*, and PAO1Δ*pilB*Δ*pilT*Δ*pilU* and assayed them for TM, pilin production, and surface pili. We reasoned that in these sensitized genetic backgrounds, in which pilus retraction has been disabled, we would be able to detect any residual surface pili resulting from basal PilB activity. All triple mutants were defective for TM (Fig. 4A and B). Detectable levels of surface pili were found for PAO1Δ*chpA*Δ*pilT*Δ*pilU* and PAO1Δ*pilG* Δ*pilT*Δ*pilU*, but not PAO1Δ*pilB*Δ*pilT*Δ*pilU* (Fig. 4C). These data indicate that PilB-dependent extension occurs in the absence of signaling input from either ChpA or PilG and that PilB is absolutely required for pilus extension.

PilH enhances the function of PilT but not that of PilU. PAO1Δ*pilT*$^{\text{CTX-}pilU}$ is defective for TM and has increased levels of surface piliation relative to the WT, Δ*pilH*, and Δ*pilU* strains (Fig. 3C). If PilH is involved in mediating PilT or PilU activity, we would predict that PAO1Δ*pilH*Δ*pilT*$^{\text{CTX-}pilU}$ and PAO1Δ*pilH*Δ*pilU* should recapitulate the phenotypes of PAO1Δ*pilT*$^{\text{CTX-}pilU}$ and PAO1Δ*pilU*, respectively. To test this prediction, we constructed PAO1Δ*pilH*Δ*pilT*$^{\text{CTX-}pilU}$ and PAO1 Δ*pilH*Δ*pilU* and assayed them for TM, pilin production, surface pili, and phage sensitivity.

PAO1Δ*pilH*Δ*pilT*$^{\text{CTX-}pilU}$ was defective in TM, similar to PAO1Δ*pilT*$^{\text{CTX-}pilU}$, and was clearly distinguishable from the intermediate TM of PAO1Δ*pilH* (Fig. 5A and B). PAO1 Δ*pilH*Δ*pilT*$^{\text{CTX-}pilU}$ was resistant to phage PO4 infection (Table 3), suggesting that PilH and PilT function in the same pathway. PAO1Δ*pilH*Δ*pilT*$^{\text{CTX-}pilU}$ reproducibly showed significantly increased levels of surface pili relative to PAO1Δ*pilH* and PAO1Δ*pilT*$^{\text{CTX-}pilU}$ ($P < 0.05$, Fig. 5C and D). These data suggest that PilH enhances the retractile activity of PilT and that some additional retractile activity, enhanced perhaps by PilH, must be present.

PAO1Δ*pilH*Δ*pilU* had a TM phenotype indistinguishable from that of the Δ*pilU* strain (Fig. 5A and B), resembled the Δ*pilH* strain in its unusual plaque morphology when infected with phage PO4 (Table 3), and had increased levels of surface pili relative to the Δ*pilU* strain (Fig. 5C and D). The simplest interpretation of these results is that both PilH and PilU regulate TM, but that they do not operate in the same pathway to mediate retraction. The conclusion that PilU does not appear to function in pilus retraction is further supported by exami-

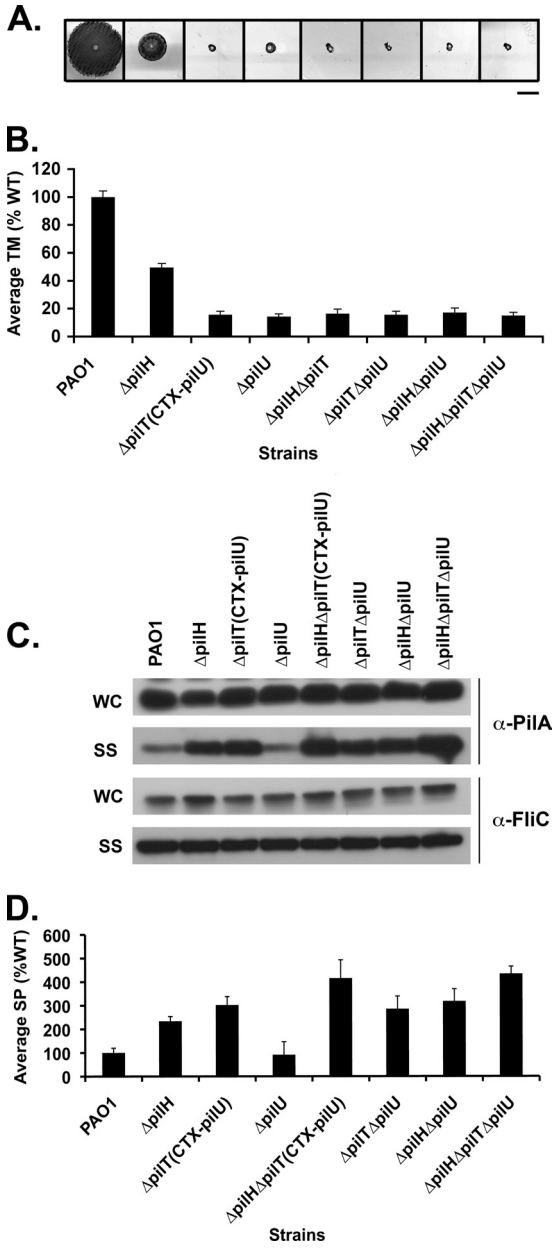

FIG. 5. PilH enhances the function of PilT but not PilU. (A) Subsurface TM assays were performed as described in Fig. 1. Bar, 1 cm. (B) Graph depicting average TM zone diameters for the indicated strains. Shown are the means ± the SD ($n = 5$). The residual zone of TM in all of the mutants represents colony growth and is similar to that of the Δ*pilA* mutant. (C) A 1:5 dilution of surface structures (SS) and cell intracellular (WC) preparations of the indicated strains were immunoblotted with a polyclonal antibody to PilA (α-pilA) or to FliC (α-FliC), as described in Fig. 2. (D) Quantification of surface piliation levels relative to a FliC loading control. Surface piliation levels are expressed as a percentage of PAO1. Shown are the means ± the SD ($n = 3$).

nation of PAO1Δ*pilT*Δ*pilU* and PAO1Δ*pilH*Δ*pilT*Δ*pilU*. Δ*pilT* Δ*pilU* had surface piliation levels similar to those of PAO1 Δ*pilT*$^{\text{CTX-}pilU}$ (Fig. 5C and D). Likewise, PAO1Δ*pilH*Δ*pilT* Δ*pilU* had surface piliation levels similar to those of PAO1 Δ*pilH*Δ*pilT*$^{\text{CTX-}pilU}$ (Fig. 5C and D). Thus, the loss of PilU function did not further increase the amount of surface pili, suggesting that the additional retractile activity is not encoded by *pilU*.

The phosphoacceptor sites of PilG and PilH are required for their function. Our results thus far support a model in which the CheY-like response regulator proteins PilG and/or PilH are targets of ChpA kinase activity, suggesting that their ability to be phosphorylated is required for function. To test this hypothesis, we constructed strains in which we replaced the WT allele on the chromosome with either His-tagged *pilG* or *pilH* (*pilG*-His, *pilH*-His) or His-tagged *pilG* and *pilH* derivatives in which the putative phosphoacceptor site aspartate residues were replaced with alanine residues [*pilG*(D58A)-His and *pilH*(D52A)-His]. The various strains were assayed for TM, pilin production, and surface pili. The *pilG*-His strain showed no defect in TM, intracellular pilin levels, or surface piliation (Fig. 6), suggesting that the His tag did not interfere with function of PilG. In the case of the *pilH*-His strain, the epitope tag slightly decreased its function, as the strain carrying the His-tagged protein showed slightly decreased TM relative to WT (Fig. 6) and increased surface piliation, although not nearly to the same extent as Δ*pilH*.

Consistent with the idea that signaling through PilG and PilH is required for their function, the phenotypes of the PAO1Δ*pilG*(D58A)-His or PAO1Δ*pilH*(D52A)-His strains were indistinguishable from those of the Δ*pilG* and Δ*pilH* strains, respectively. PAO1Δ*pilG*(D58A)-His was deficient for TM and lacked surface pili (Fig. 6A). PAO1Δ*pilH*(D52A)-His had an intermediate TM phenotype, increased surface pili, and formed aberrant plaques (Fig. 6 and Table 3). We were unable to detect His-tagged wild-type or mutant PilG or PilH by immunoblot analysis in either soluble or total cell lysates. Therefore, it is not possible to formally rule out that the defects observed in TM and surface piliation for PAO1Δ*pilG*(D58A)-His and PAO1Δ*pilH*(D52A)-His were secondary to reduced protein levels. We consider this extremely unlikely, however, since the equivalent point mutation has been made in many other CheY homologs without affecting protein levels or protein stability (23, 24, 38).

The histidine kinase domain of ChpA is required for function. To test whether the histidine kinase activity of ChpA is required for its function, we mutated the histidine kinase domain. Although histidine kinase mutants are typically constructed by altering the histidine residue that is the target of autophosphorylation (20), this approach is not possible for ChpA, since it encodes eight potential sites of phosphorylation (six histidine-containing phosphotransfer domains and two novel serine- and threonine-containing phosphotransfer domains [55]). Instead, we mutated the signature DXG motif of the G1 box of a chromosomal FLAG-tagged *chpA* derivative to AAA. The G1 box, along with the G2 box, is implicated in the binding and hydrolysis of ATP (21). *E. coli cheA* in which the DXG motif of the G1 box has been altered fails to autophosphorylate, shows decreased affinity for ATP *in vitro*, and is deficient for chemotaxis *in vivo* (15, 21). ChpA was C-terminally fused to FLAG so that levels of the wild-type and mutant protein could be compared.

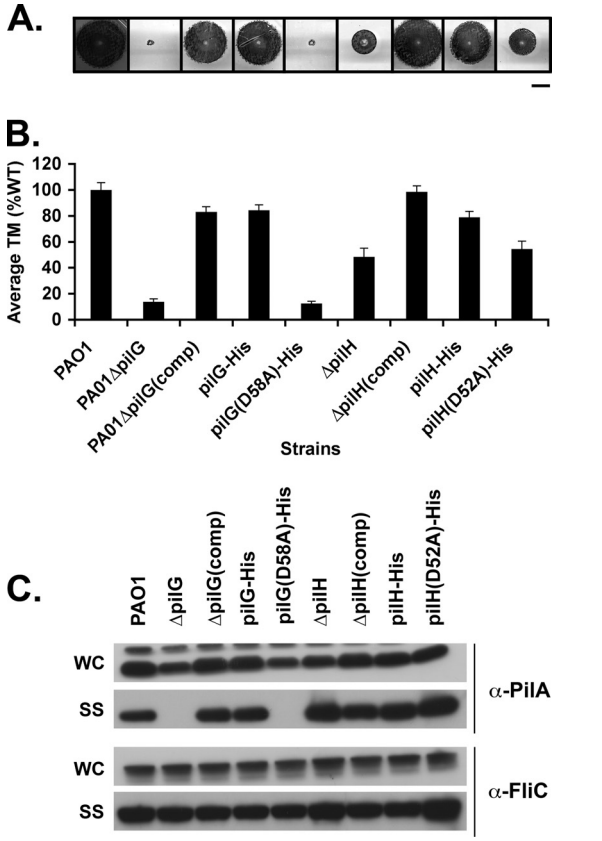

FIG. 6. The phosphoacceptor sites of PilG and PilH are required for function. (A) Subsurface TM assays of PAO1 (WT) and the Δ*pilG*, Δ*pilG*(comp), Δ*pilH*, Δ*pilH*(comp), His-tagged *pilG* (*pilG*-His), and *pilH* (*pilH*-His) mutants, as well as the His-tagged *pilG* and *pilH* point mutant strains PAO1Δ*pilG*(D58A)-His and PAO1Δ*pilH*(D52A)-His. Bar, 1 cm. (B) Graph depicting average TM zone diameters for the indicated strains. Shown are the means ± the SD ($n = 5$). The residual zone of TM in the *pilG* mutants represents colony growth and is similar to that of the Δ*pilA* mutant. (C) Surface structures (SS) and intracellular (WC) preparations of the indicated strains were immunoblotted with a polyclonal antibody to PilA (α-pilA) or to FliC (α-FliC), as described in Fig. 2.

We assayed the PAO1Δ*chpA*-FLAG and PAO1 Δ*chpA*(AAA)-FLAG strains for TM, intracellular pilin levels, and surface piliation. PAO1Δ*chpA*-FLAG was indistinguishable from the WT in all assays (Fig. 7A, B, and C), suggesting that the FLAG tag does not interfere with ChpA function. In contrast, the PAO1Δ*chpA*(AAA)-FLAG histidine kinase mutant exhibited a phenotype similar to that of PAO1Δ*chpA*. It was defective for TM, had slightly reduced levels of intracellular pilin, and had greatly reduced surface pili (Fig. 7A, B, and C). Immunoblots with α-FLAG showed equal production of ChpA-FLAG and ChpA(AAA)-FLAG, indicating that the defects in pilin function in the ChpA histidine kinase mutant was not due decreased protein levels (Fig. 7D). ChpA-FLAG and ChpA(AAA)-FLAG proteins were only detectable in the insoluble cell lysate fraction (Fig. 7D and data not shown), suggesting that ChpA may be membrane bound. In support of this idea, the TMpred program, which can be used to identify

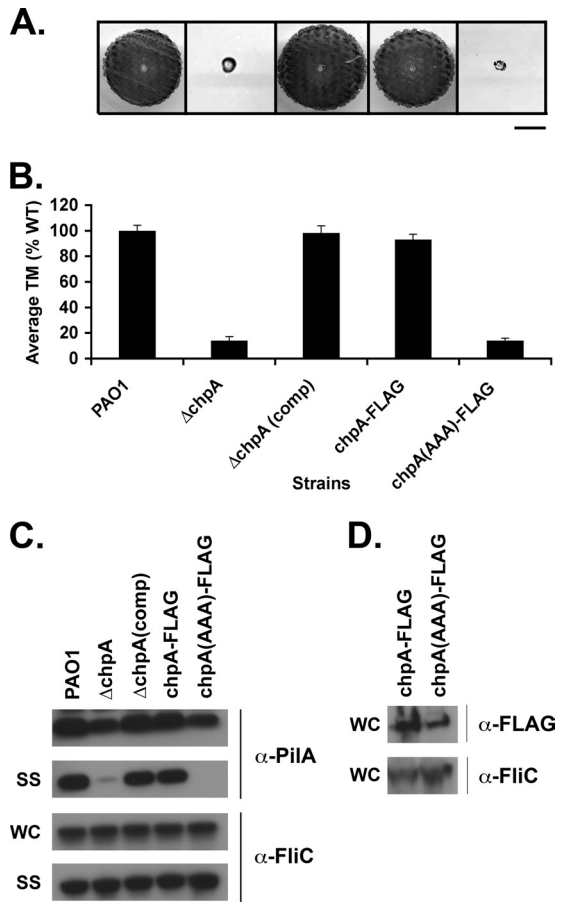

FIG. 7. The histidine kinase domain of ChpA is required for function. (A) Subsurface TM assay of PAO1 (WT) and the Δ*chpA*, Δ*chpA*(comp), and FLAG-tagged *chpA* (*chpA*-FLAG) mutants, as well as the FLAG-tagged *chpA* histidine kinase mutant [*chpA*(AAA)-FLAG]. Bar, 1 cm. (B) Graph depicting average TM zone diameters for the indicated strains. Shown are the means ± the SD ($n = 5$). The residual zone of TM in the *ChpA* mutants represents colony growth and is similar to that of the Δ*pilA* mutant. (C) Surface structures (SS) and intracellular (WC) preparations of the indicated strains were immunoblotted with a polyclonal antibody to PilA (α-pilA) or to FliC (α-FliC), as described in Fig. 2. (D) Levels of ChpA-FLAG and ChpA(AAA)-FLAG. To prepare protein samples, cells were harvested from 2 ml of culture grown shaking for 16 h at 37°C, resuspended in 400 μl of SDS-PAGE sample buffer, passaged through a 27.5 gauge needle three times, and boiled for 5 min. Then, 10% of the total sample volumes were separated by SDS-PAGE and immunoblotted with 2.5 μg of α-FLAG M2 monoclonal antibody/ml.

potential transmembrane regions and orientations, strongly predicts three transmembrane domains for ChpA (data not shown). These data provide genetic evidence that the histidine kinase domain of ChpA is required for its function.

The Chp system may functionally regulate *pilA* transcription by controlling pilus extension and retraction. Immunoblot analysis of the Δ*chpA*, Δ*pilG*, and Δ*pilB* cell lysates shows an ~2-fold decrease in intracellular pilin levels relative to WT (Fig. 2C). To determine whether this defect occurred at the level of *pilA* transcription, a P_{pilA}-*lacZ* transcriptional fusion reporter was constructed. The construct contained 500 bp of sequence upstream of the *pilA* start codon, which should be sufficient to include all *cis*-regulatory sequences required for *pilA* transcription (25, 26, 30, 32). This reporter fusion was integrated at the CTX site (4) in various mutant strain backgrounds. For bacteria cultured on solid media, *pilA* transcription is increased ~2-fold in the Δ*pilA* strain compared to the WT (Fig. 8A; $P < 0.05$), suggesting that PilA may serve as a negative regulator of *pilA* transcription. Unexpectedly, β-galactosidase activity was reduced by ca. 90 to 95% relative to the WT in Δ*chpA*, Δ*pilG*, and Δ*pilB*::CTX-P_{pilA}-*lacZ* reporter strains when assayed from bacteria cultured on solid media (Fig. 8A; $P < 0.05$).

As a negative control, we constructed an in-frame deletion in *pilR*, the response regulator in the PilR/PilS two-component regulatory system which, along with σ^{54}, is required for *pilA* transcription (25, 26, 30, 32). Although the defects in *pilA* transcription in the Δ*chpA*, Δ*pilG*, and Δ*pilB* strains do not appear as severe as in the Δ*pilR* strain, where the levels of transcription are similar to a promoterless *lacZ* gene incorporated at the CTX site (CTX-*lacZ*, Fig. 8A), they are not statistically different from the Δ*pilR* strain. *pilA* transcription was slightly decreased in a Δ*fliC* background (Fig. 8A). Our finding that intracellular pilin levels are only decreased twofold in the Δ*chpA*, Δ*pilG*, and Δ*pilB* strains, whereas *pilA* transcription is decreased 90 to 95%, suggests the possibility that intracellular levels of PilA may also be regulated posttranscriptionally.

We next measured *pilA* transcription in the Δ*pilH*, Δ*pilT*, and Δ*pilU* strains. Since the CTX site of PAO1Δ$pilT^{CTX\text{-}pilU}$ already contained an exogenous gene (*pilU*), we constructed a PilT mutant (PAO1$pilT^{Trunc}$) missing the first 143 amino acids of the protein but which retained the 783 bp upstream of PilU, including the presumptive upstream regulatory sequences necessary for *pilU* production. We introduced the P_{pilA}-*lacZ* reporter construct into the CTX site of $pilT^{Trunc}$. This mutant is defective for TM, has increased surface pili, and could be complemented for TM by expression of *pilT* in *cis* or in *trans* (data not shown). $pilT^{Trunc}$ reproducibly showed a 40% increase in β-galactosidase activity relative to WT when assayed from bacteria cultured on solid media (Fig. 8A; $P < 0.05$), a finding consistent with the notion that pilin disassembly or intracellular pilin levels may regulate pilin transcription. *pilA* promoter activity was unchanged relative to the WT in the Δ*pilU* strain, further supporting the idea that PilU does not function in retraction. *pilA* transcription in the PAO1 Δ*pilH*::CTX-P_{pilA}-*lacZ* reporter strain, which is hyperpiliated, was reduced to 15% of WT, similar to the levels observed for the Δ*chpA*, Δ*pilG*, and Δ*pilB* strains (Fig. 8A). In addition to its role in mediating pilus retraction, it is possible that PilH may have a positive role in regulating *pilA* transcription.

We investigated and compared *pilA* transcription in WT and mutant strains cultured in liquid media. For WT PAO1, the levels of *pilA* transcription were decreased by ca. 95% for cells grown in liquid culture to stationary phase compared to cells cultured on solid media (Fig. 8A; $P < 0.0001$). This finding suggests that *pilA* transcription is highly repressed in WT cells cultured in liquid media. Furthermore, given that the intracellular and surface pilin levels were similar under the two different growth conditions (Fig. 8C), these results suggest that the turnover of pilin is much slower in cells cultured in liquid compared to on solid media. Nonetheless, even in liquid culture, *pilA* transcription was increased 27-fold relative to WT in the Δ*pilA* background (Fig. 8B, $P < 0.05$). The absolute levels

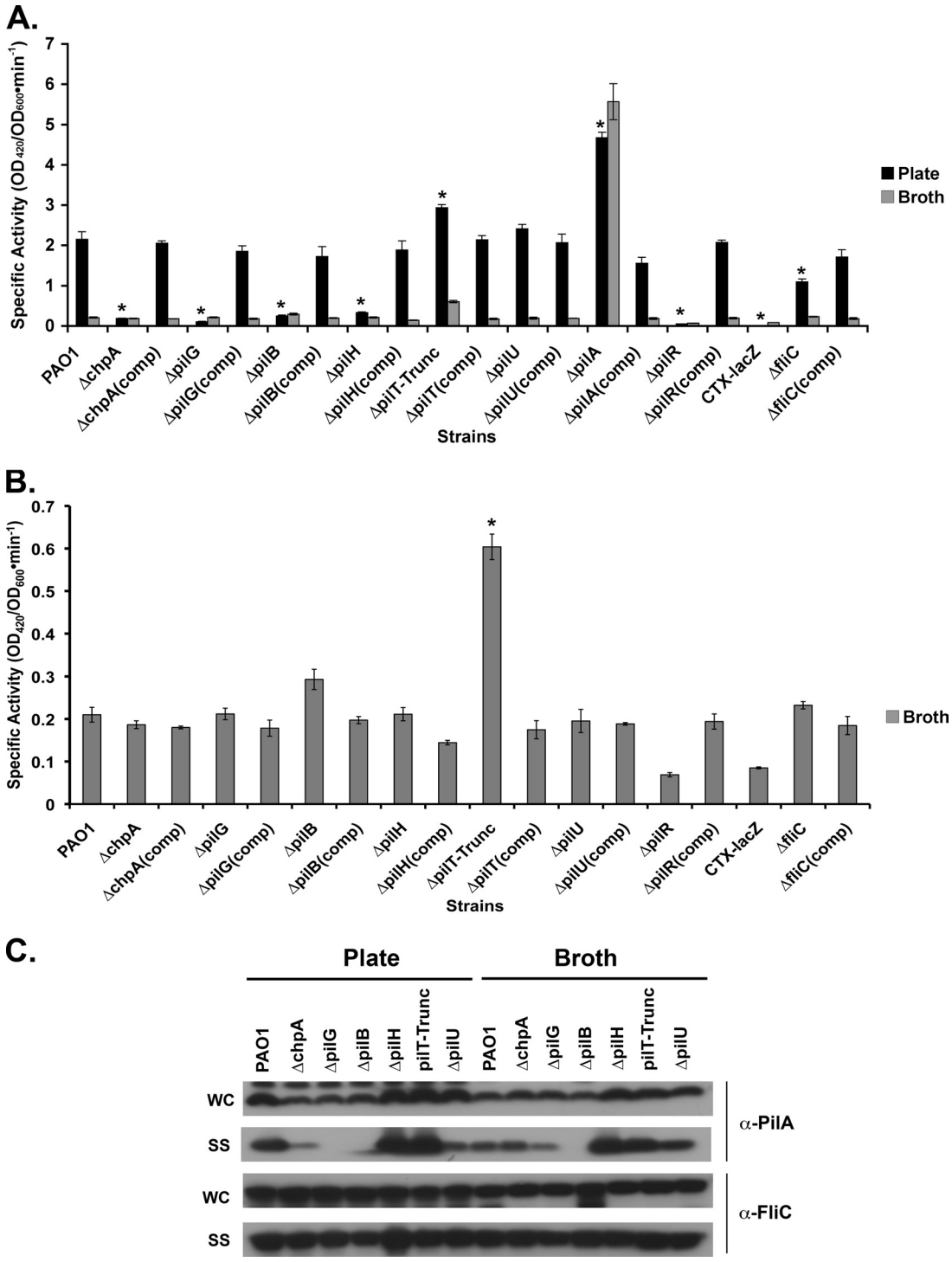

FIG. 8. The Chp system regulates *pilA* transcription by mediating intracellular levels of PilA. (A) The indicated strains harboring the P_{pilA}-*lacZ* fusion and PAO1 harboring a promoterless *lacZ* gene (CTX-*lacZ*) integrated into the chromosome at the *attB* site were cultured in liquid (A and B) or on solid (A) medium for 16 h. The β-galactosidase activity of samples was measured, and the specific activities relative to the OD_{600} were calculated. Shown are the means ± the SD ($n = 3$). *, $P < 0.05$. (C) Surface structures (SS) and intracellular (WC) preparations of the indicated strains cultured in liquid (broth) or on solid (plate) medium were immunoblotted with a polyclonal antibody to PilA (α-pilA) or to FliC (α-FliC), as described in Fig. 2. The higher-molecular-weight band above pilin in the whole-cell lysates represents a cross-reactive band present in all samples.

of *pilA* transcription for broth- and plate-cultured bacteria in the Δ*pilA* background were similar, suggesting that pilin functions as a negative regulator under both culture conditions and that *pilA* transcription was maximally derepressed in the absence of PilA.

Similar to PAO1*pilT*$^{\text{Trunc}}$ bacteria cultured on solid media, the PAO1*pilT*$^{\text{Trunc}}$ strain cultured in broth had increased levels of surface pili and showed a threefold increase in *pilA* transcription compared to the WT (Fig. 8A and B; $P < 0.05$). The observation that PAO1*pilT*$^{\text{Trunc}}$ shows a moderate increase in β-galactosidase activity suggests that pili remain functional under liquid culture conditions and, as such, PilT continues to act as a functional regulator of *pilA* transcription by mediating intracellular levels of PilA. Similarly, the hyperpiliated phenotype of Δ*pilH* suggests a role in regulating pilus retraction in liquid as on solid media (Fig. 8C).

We did not detect decreases in *pilA* transcription for mutants defective in pilin export (i.e., the Δ*chpA*, Δ*pilG*, and Δ*pilB* mutants) under liquid culture conditions (Fig. 8B). Of interest, the levels of intracellular and surface pilin in Δ*chpA* and Δ*pilG* mutants were similar to those of the WT, suggesting that the role they play in the regulation of pilus dynamics may be culture condition specific (Fig. 8B). The Δ*pilB* mutant, however, lacks detectable surface pili when assayed from plates or out of broth, underscoring its essential role in controlling pilus extension (Fig. 8C). Unlike on solid media, however, the Δ*pilB* mutant export defect does not correspond to a decrease in intracellular pilin levels or in *pilA* transcription (Fig. 8B). Similarly, an apparent increase in pilin production in the Δ*pilH* strain does not correspond to increased *pilA* transcription (Fig. 8B). Some of these inconsistencies may be due, in part, to the global decrease in *pilA* transcription in cells cultured in liquid compared to on solid media, a finding that may be indicative of an overall decrease in pilus activity under liquid culture condition and which may make subtle changes in levels of *pilA* transcription difficult to detect.

DISCUSSION

P. aeruginosa uses Tfp for locomotion, adherence, and biofilm formation during growth in diverse environments. We have previously described the initial characterization of the Chp signaling system, a putative chemosensory system that regulates Tfp function and biofilm formation (3, 55). In the present study, we used genetic analysis to further understand the mechanism by which the Chp system controls Tfp function. We present data consistent with the hypothesis that PilA is a negative regulator of *pilA* transcription and that the Chp system, along with the ATPases PilB and PilT, serves to functionally regulate *pilA* transcription by modulating intracellular levels of PilA.

Through the construction and complementation of in-frame deletion mutants, we have confirmed the role of ChpA, PilG, and PilB in the regulation of pilus extension and the role of PilH and PilT in retraction. Our extensive analysis of Tfp phenotypes of double and triple mutants in factors involved in extension (*chpA*, *pilG*, and *pilB*) and those involved in retraction (*pilH* and *pilT*) suggest that factors involved in extension function upstream of those involved in retraction. Furthermore, our data indicate that while PilB is absolutely required for pilus extension, it retains some extension activity in the absence of upstream signaling input from either ChpA or PilG. Our data also indicate that PilH enhances PilT activity and that PilT retains some retractile activity in the absence of PilH.

It is intriguing, although not without precedence (51), that the Chp system uses two CheY-like proteins, PilG and PilH, to influence ATPase function, though the exact mechanism remains to be elucidated. These response regulators could affect association of PilB or PilT with the inner membrane components of the pilus system. Alternatively, they could promote PilB or PilT hexamer formation, or they could affect PilB or PilT turnover or polar localization. Whether these two response regulators compete for phosphorylation or have distinct subcellular localization will also be of interest to investigate in the future.

Our data present conflicting evidence for the role of PilU in mediating pilus retraction. PilU is a member of the family of hexameric secretion ATPases and demonstrates ATPase activity *in vitro* (8), has a high degree of homology to PilT (39% identical and 61% similar), and likely arose by gene duplication (56). Like PAO1Δ*pilT*$^{\text{CTX-}pilU}$, PAO1Δ*pilU* is severely defective in TM, but it is phage sensitive and thus retains some retractile function (56; the present study). The most straightforward model is that PilU functions as an accessory retractile motor to PilT. Indeed, older published electron microscopy data show hyperpiliation of a *pilU* insertion mutant (56), suggesting a role for PilU in retraction, though surface pili levels were not measured.

In support of an accessory role for PilU in pilus retraction, we observed (i) that PAO1Δ*pilH*Δ*pilT* exhibited increased surface piliation relative to PAO1Δ*pilH* and PAO1Δ*pilT*$^{\text{CTX-}pilU}$; (ii) that residual surface piliation due to basal PilB activity is only apparent in a Δ*pilG* background when both *pilT* and *pilU* are deleted (i.e., PAO1Δ*pilG*Δ*pilT*Δ*pilU*); and (iii) that the levels of surface piliation in strain PAO1Δ*chpA*Δ*pilTpilU* are clearly increased relative to strains PAO1Δ*chpA* and PAO1Δ*chpA*Δ*pilT*$^{\text{CTX-}pilU}$. However, if PilU has retractile activity, even if minor, we would predict that the PAO1Δ*pilT*Δ*pilU* strain would have increased surface piliation relative to PAO1Δ*pilT*$^{\text{CTX-}pilU}$. What we observed, however, is that the degree of surface piliation for PAO1Δ*pilT*Δ*pilU* is the same as that for PAO1Δ*pilT*$^{\text{CTX-}pilU}$ and that the surface piliation of PAO1Δ*pilH*Δ*pilT*Δ*pilU* is similar to that of PAO1 Δ*pilH*Δ*pilT*$^{\text{CTX-}pilU}$. It remains to be determined whether the number or the length of the pili differ or whether their spatial distribution is altered in these mutants. Nonetheless, these observations suggest an additional PilH-dependent retraction factor that is not PilU.

We show for the first time that the histidine kinase domain of ChpA is essential for Tfp function. ChpA is one of the most complex CheA homologs yet to be described. In addition to its histidine kinase domain, it possesses eight potential sites of phosphorylation and a CheY-like receiver domain at its C terminus. Previous studies have demonstrated that the second and third Hpt domains contribute to TM, while the CheY domain is absolutely essential; a potential role in the regulation of swarming motility has also been shown for Hpt4 and Hpt5 (37). It is possible that the ChpA histidine kinase domain catalyzes the autophosphorylation of Hpt2 and/or Hpt3, which then transfers phosphate to the C-terminal CheY domain. Al-

ternatively, the phosphates may be transferred to PilG and/or PilH, which may compete with the CheY domain for phosphorylation. A combination of biochemical and genetic analyses will be required to further elucidate this complex signaling pathway. ChpA may have an additional role in the regulation of type III secretion. β-Galactosidase assays show decreased transcription of the type III secreted effector *exoT*, and microarray analysis suggests that ChpA plays some role in the regulation of expression of the type III secretion system (our unpublished data). How this regulation occurs and whether it is dependent upon the N-terminal domain of ChpA, which is homologous to FimL, a known regulator of type III secretion (53), or upon ChpA signaling, remains to be determined.

Our studies suggest a role for Tfp dynamics in regulating *pilA* transcription. First, we found that *pilA* transcription is much lower in WT bacteria cultured in liquid compared to bacteria grown on solid media, despite the fact that the amount of intracellular and surface pili is the same under both conditions. This finding suggests that pilin turnover is decreased in liquid-grown cultures relative to plate-grown cultures and may correlate with a decreased need for pilus pilus retraction or extension in liquid culture conditions. Second, in the absence of PilA or in the absence of retraction, *pilA* transcription is increased, suggesting that unassembled pilin subunits may function as a negative regulator of *pilA* transcription. Specifically, we observed a twofold increase in *pilA* transcription in Δ*pilA* and a reproducible but smaller increase in transcription in a *pilT* mutant. When we attempted to overproduce PilA by expression from a plasmid-borne copy of *pilA* under an inducible promoter, we were unable to increase pilin levels or to affect transcription from the native *pilA* promoter driving *lacZ* (unpublished data). Our data are consistent with previous reports that showed negative-feedback regulation of *pilA* transcription by PilA in *P. aeruginosa* (16) and in *M. xanthus* (29, 58), where it is postulated that unassembled pilin subunits are sensed by the PilR/PilS two-component regulatory system (29). Whitchurch and Mattick (56), in contrast, reported Northern blot analysis demonstrating decreased *pilA* mRNA in *pilT* or *pilU* insertion mutants. Third, our data suggest that the Chp system, along with the ATPases PilB and PilT, serves to functionally regulate *pilA* transcription by modulating intracellular levels of PilA. Specifically, we show that mutants with defects in PilA export (i.e., Δ*chpA*, Δ*pilB*, and Δ*pilG* mutants) have decreased *pilA* transcription, whereas a mutant defective in pilin disassembly (PAO1Δ$pilT^{Trunc}$) demonstrated increased *pilA* transcription. Similarly, Johnson et al. (31) showed that *pilA* transcription by both Northern analysis and *lacZ* assay was upregulated in hyperpiliated mutants and downregulated in hypopiliated mutants. Our data are consistent with observations made in other organisms, such as the cyanobacterium *Synechocystis* sp. strain PCC6803 and *Neisseria gonorrhea*, where hyperpiliated *pilT* mutants have been shown to accumulate higher than normal levels of *pilA1* transcript (5, 14). One attractive model is that as the pilus is dissembled, PilS senses pilin levels associated with the inner membrane and regulates PilR activity and *pilA* transcription.

We note that transposon insertion mutations in *pilG* and other Chp system components (*pilH*, *pilI*, and *pilJ*) have been reported to have WT levels of *pilA* transcription in strain PAK (12, 13), although at least one *chpA* insertion mutant has been shown to have a defect in *pilA* transcription (55). Point mutations to an Hpt domain (H1088Q) and the *cheY* domain (D2406N) of *chpA* resulted in increased *pilA* transcription by Northern analysis (37). The reason for the discrepancy between the insertion mutant, PAO1Δ*chpA*, and the point mutants remains to be determined; it may reflect strain differences or differences in culture conditions. It is also unclear if the increase in *pilA* transcription in the *chpA* point mutants corresponds to increased surface piliation. Mutations in components of other putative chemosensory systems proposed to regulate Tfp-driven motility have been shown to have defects in *pilA* transcription (57).

Our studies suggest that PilH regulates pathways in addition to pilin retraction, suggesting that this CheY homolog interfaces with multiple signal transduction circuits. The Δ*pilH* mutant has aberrant TM and increased surface pili. Based on its hyperpiliation phenotype, we would predict that the *pilH* mutant would show increased levels of *pilA* transcription; however, it is actually reduced to levels near those of the Δ*chpA*, Δ*pilG*, and Δ*pilB* mutants, suggesting that *pilH* may play some additional, positive role in regulating *pilA* transcription. Unique among the Chp system mutants, PAO1Δ*pilH* also shows altered pyocyanin and rhamnolipid production that correspond to changes in *phzA1* and *rhlA* transcription and increased virulence in a *Drosophila* infection model (our unpublished data). Site-directed *pilH* mutants, in which the aspartate residue in the putative phosphoacceptor site is replaced with alanine, recapitulate the virulence factor production phenotypes of the null mutant (our unpublished data). Further studies will need to be carried out to determine the full range of PilH function.

The data presented here provides genetic evidence consistent with a model in which ChpA acts as a histidine kinase to phosphorylate PilG and/or PilH. PilG-P, in turn, modulates PilB to drive pilus extension, and PilH-P modulates PilT to drive pilus retraction (Fig. 1). Future studies will focus on complementing these genetic studies with biochemical analysis. The ability of ChpA to autophosphorylate, and on which of its eight potential phosphorylation sites, and to participate in phospho-transfer reactions with PilG, PilH, or its own CheY domain has yet to be demonstrated *in vitro*. Moreover, direct interactions between ChpA and PilG, ChpA and PilH, PilG and PilB, and PilH, and PilT/PilU remain to be shown. These interactions may be more complex than we previously imagined. A recent study demonstrated direct binding of PilZ and FimX, two proteins previously shown to have roles in the regulation of Tfp function, to PilB (19). Whether and how PilG interacts with this complex remains to be determined. It is also unclear whether a similar or completely novel complex exists for PilT and whether and how PilH might interact with those components of the retraction apparatus.

ACKNOWLEDGMENTS

We thank Carol Gross, Cynthia Whitchurch, and current and past members of the Engel lab for discussion and comments. We thank Lori Burrows, Daniel Wozniak, and Rebecca Wilson for the generous donation of reagents.

This study was supported by NIH grant R01 AI42806 (J.N.E.).

REFERENCES

1. **Alm, R., and J. S. Mattick.** 1995. Identification of a gene, *pilV*, required for type 4 fimbrial biogenesis in *Pseudomonas aeruginosa*, whose product possesses a pre-pilin-like leader sequence. Mol. Microbiol. **16:**485–496.
2. **Baker, M. D., P. M. Wolanin, and J. B. Stock.** 2006. Signal transduction in bacterial chemotaxis. Bioessays **28:**9–22.
3. **Barken, K. B., S. J. Pamp, L. Yang, M. Gjermansen, J. J. Bertrand, M. Klausen, M. Givskov, C. B. Whitchurch, J. N. Engel, and T. Tolker-Nielsen.** 2008. Roles of type IV pili, flagellum-mediated motility and extracellular DNA in the formation of mature multicellular structures in *Pseudomonas aeruginosa* biofilms. Environ. Microbiol. **10:**2331–2343.
4. **Becher, A., and H. P. Schweizer.** 2000. Integration-proficient *Pseudomonas aeruginosa* vectors for isolation of single-copy chromosomal *lacZ* and *lux* gene fusions. Biotechniques **29:**948–952.
5. **Bhaya, D., N. R. Bianco, D. Bryant, and A. Grossman.** 2000. Type IV pilus biogenesis and motility in the cyanobacterium *Synechocystis* sp. PCC6803. Mol. Microbiol. **37:**941–951.
6. **Bradley, D. E., and T. L. Pitt.** 1974. Pilus-dependence of four *Pseudomonas aeruginosa* bacteriophages with non-contractile tails. J. Gen. Virol. **23:**1–15.
7. **Chiang, P., and L. L. Burrows.** 2003. Biofilm formation by hyperpiliated mutants of *Pseudomonas aeruginosa*. J. Bacteriol. **185:**2374–2378.
8. **Chiang, P., L. M. Sampaleanu, M. Ayers, M. Pahuta, P. L. Howell, and L. L. Burrows.** 2008. Functional role of conserved residues in the characteristic secretion NTPase motifs of the *Pseudomonas aeruginosa* type IV pilus motor proteins PilB, PilT, and PilU. Microbiology **154:**114–126.
9. **Cosson, P., L. Zulianello, O. Join-Lambert, F. Faurisson, L. Bebbie, M. Benghezal, C. van Delden, L. K. Curty, and T. Kohler.** 2002. *Pseudomonas aeruginosa* virulence analyzed in a *Dictyostelium discoideum* host system. J. Bacteriol. **184:**3027–3033.
10. **Costerton, J. W., P. S. Stewart, and E. P. Greenberg.** 1999. Bacterial biofilms: a common cause of persistent infections. Science **284:**1318–1322.
11. **D'Argenio, D. A., L. A. Gallagher, C. A. Berg, and C. Manoil.** 2001. *Drosophila* as a model host for *Pseudomonas aeruginosa* infection. J. Bacteriol. **183:**1466–1471.
12. **Darzins.** 1993. The *pilG* gene product, required for *Pseudomonas aeruginosa* pilus production and twitching motility, is homologous to the enteric, single domain response regulator CheY. J. Bacteriol. **175**:5934–5944.
13. **Darzins, A.** 1994. Characterization of a *Pseudomonas aeruginosa* gene cluster involved in pilus biosynthesis and twitching motility: sequence similarity to the chemotaxis proteins of enterics and the gliding bacterium *Myxococcus xanthus*. Mol. Microbiol. **11:**137–153.
14. **Dietrich, M., H. Mollenkopf, M. So, and A. Friedrich.** 2009. Pilin regulation in the pilT mutant of *Neisseria gonorrhoeae* strain MS11. FEMS Microbiol. Lett. **296:**248–256.
15. **Ellefson, D. D., U. Weber, and A. J. Wolfe.** 1997. Genetic analysis of the catalytic domain of the chemotaxis-associated histidine kinase CheA. J. Bacteriol. **179:**825–830.
16. **Elleman, T. C., P. A. Hoyne, D. J. Stewart, N. M. McKern, and J. E. Peterson.** 1986. Expression of pili from *Bacteroides nodosus* in *Pseudomonas aeruginosa*. J. Bacteriol. **168:**574–580.
17. **Engel, J. N.** 2003. Molecular pathogenesis of acute *Pseudomonas aeruginosa* infections, p. 201–230. *In* A. Hauser and J. Rello (ed.), Severe infections caused by *Pseudomonas aeruginosa*. Kluwer Academic/Plenum Press, New York, NY.
18. **Garrett, E. S., D. Perlegas, and D. J. Wozniak.** 1999. Negative control of flagellum synthesis in *Pseudomonas aeruginosa* is modulated by the alternative sigma factor AlgT (AlgU). J. Bacteriol. **181:**7401–7404.
19. **Guzzo, C. R., R. K. Salinas, M. O. Andrade, and C. S. Farah.** 2009. PILZ protein structure and interactions with PILB and the FIMX EAL domain: implications for control of type IV pilus biogenesis. J. Mol. Biol. **393:**848–866.
20. **Hess, J. F., K. Oosawa, N. Kaplan, and M. I. Simon.** 1988. Phosphorylation of three proteins in the signaling pathway of bacterial chemotaxis. Cell **53:**79–87.
21. **Hirschman, A., M. Boukhvalova, R. VanBruggen, A. J. Wolfe, and R. C. Stewart.** 2001. Active site mutations in CheA, the signal-transducing protein kinase of the chemotaxis system in *Escherichia coli*. Biochemistry **40:**13876–13887.
22. **Hoang, T. T., A. J. Kutchma, A. Becher, and H. P. Schweizer.** 2000. Integration-proficient plasmids for *Pseudomonas aeruginosa*: site-specific integration and use for engineering of reporter and expression strains. Plasmid **43:**59–72.
23. **Inclan, Y. F., S. Laurent, and D. R. Zusman.** 2008. The receiver domain of FrzE, a CheA-CheY fusion protein, regulates the CheA histidine kinase activity and downstream signaling to the A- and S-motility systems of *Myxococcus xanthus*. Mol. Microbiol. **68:**1328–1339.
24. **Inclan, Y. F., H. C. Vlamakis, and D. R. Zusman.** 2007. FrzZ, a dual CheY-like response regulator, functions as an output for the Frz chemosensory pathway of *Myxococcus xanthus*. Mol. Microbiol. **65:**90–102.
25. **Ishimoto, K. S., and S. Lory.** 1989. Formation of pilin in *Pseudomonas aeruginosa* requires the alternative σ factor (RpoN) of RNA polymerase. Proc. Natl. Acad. Sci. U. S. A. **86:**1954–1957.
26. **Ishimoto, K. S., and S. Lory.** 1992. Identification of pilR, which encodes a transcriptional activator of the *Pseudomonas aeruginosa* pilin gene. J. Bacteriol. **174:**3514–3521.
27. **Jakovljevic, V., S. Leonardy, M. Hoppert, and L. Sogaard-Andersen.** 2008. PilB and PilT are ATPases acting antagonistically in type IV pilus function in *Myxococcus xanthus*. J. Bacteriol. **190:**2411–2421.
28. **Jander, G., L. G. Rahme, and F. M. Ausubel.** 2000. Positive correlation between virulence of *Pseudomonas aeruginosa* mutants in mice and insects. J. Bacteriol. **182:**3843–3845.
29. **Jelsbak, L., and D. Kaiser.** 2005. Regulating pilin expression reveals a threshold for S motility in *Myxococcus xanthus*. J. Bacteriol. **187:**2105–2112.
30. **Jin, S., K. S. Ishimoto, and S. Lory.** 1994. PilR, a transcriptional regulator of piliation in *Pseudomonas aeruginosa*, binds to a *cis*-acting sequence upstream of the pilin gene promoter. Mol. Microbiol. **14:**1049–1057.
31. **Johnson, K., and S. Lory.** 1987. Characterization of *Pseudomonas aeruginosa* mutants with altered piliation. J. Bacteriol. **169:**5663–5667.
32. **Johnson, K., M. L. Parker, and S. Lory.** 1986. Nucleotide sequence and transcriptional initiation site of two *Pseudomonas aeruginosa* pilin genes. J. Biol. Chem. **261:**15703–15708.
33. **Kaiser, D.** 2006. A microbial genetic journey. Annu. Rev. Microbiol. **60:**1–25.
34. **Kaiser, D.** 2007. Bacterial swarming: a re-examination of cell-movement patterns. Curr. Biol. **17:**R561–R570.
35. **Klausen, M., A. Aaes-Jorgensen, S. Molin, and T. Tolker-Nielsen.** 2003. Involvement of bacterial migration in the development of complex multicellular structures in *Pseudomonas aeruginosa* biofilms. Mol. Microbiol. **50:**61–68.
36. **Klausen, M., A. Heydorn, P. Ragas, L. Lambertsen, A. Aaes-Jorgensen, S. Molin, and T. Tolker-Nielsen.** 2003. Biofilm formation by *Pseudomonas aeruginosa* wild type, flagella and type IV pili mutants. Mol. Microbiol. **48:**1511–1524.
37. **Leech, A. J., and J. S. Mattick.** 2006. Effect of site-specific mutations in different phosphotransfer domains of the chemosensory protein ChpA on *Pseudomonas aeruginosa* motility. J. Bacteriol. **188:**8479–8486.
38. **Li, Y., V. H. Bustamante, R. Lux, D. Zusman, and W. Shi.** 2005. Divergent regulatory pathways control A and S motility in *Myxococcus xanthus* through FrzE, a CheA-CheY fusion protein. J. Bacteriol. **187:**1716–1723.
39. **Mandell, G. L., J. E. Bennett, and R. Dolin.** 2005. Principles and practice of infectious diseases, 6th ed. Churchill Livingstone, Inc., New York, NY.
40. **Mattick, J. S.** 2002. Type iv pili and twitching motility. Annu. Rev. Microbiol. **56:**289–314.
41. **Merz, A. J., M. So, and M. P. Sheetz.** 2000. Pilus retraction powers bacterial twitching motility. Nature **407:**98–102.
42. **Nunn, D., S. Bergman, and S. Lory.** 1990. Products of three accessory genes, *pilB*, *pilC*, and *pilD*, are required for biogenesis of *Pseudomonas aeruginosa* pili. J. Bacteriol. **172:**2911–2919.
43. **O'Toole, G. A., and R. Kolter.** 1998. Flagellar and twitching motility are necessary for *Pseudomonas aeruginosa* biofilm development. Mol. Microbiol. **30:**295–304.
44. **Porter, S. L., G. H. Wadhams, and J. P. Armitage.** 2008. Rhodobacter sphaeroides: complexity in chemotactic signaling. Trends Microbiol. **16:**251–260.
45. **Sambrook, J., E. F. Fritsch, and T. Maniatis.** 1989. Molecular cloning: a laboratory manual. Cold Spring Harbor Laboratory Press, Cold Spring Harbor, NY.
46. **Schweizer, H. P., and T. T. Hoang.** 1995. An improved system for gene replacement and *xylE* fusion analysis in *Pseudomonas aeruginosa*. Gene **158:**15–22.
47. **Skerker, J. M., and H. C. Berg.** 2001. Direct observation of extension and retraction of type IV pili. Proc. Natl. Acad. Sci. U. S. A. **98:**6901–6904.
48. **Stover, C., X. Pham, A. Erwin, S. Mizoguchi, P. Warrener, M. Hickey, F. Brinkman, W. Hufnagle, D. Kowalik, M. Lagrou, R. Garber, L. Goltry, E. Tolentino, S. Westbrock-Wadman, Y. Yuan, L. Brody, S. Coulter, K. Folger, A. Kas, K. Larbig, R. Lim, K. Smith, D. Spencer, G. Wong, Z. Wu, and I. Paulsen.** 2000. Complete genome sequence of *Pseudomonas aeruginosa* PAO1, an opportunistic pathogen. Nature **406:**959–964.
49. **Tan, M. W., L. G. Rahme, J. A. Sternberg, R. G. Tompkins, and F. M. Ausubel.** 1999. *Pseudomonas aeruginosa* killing of *Caenorhabditis elegans* used to identify *P. aeruginosa* virulence factors. Proc. Natl. Acad. Sci. U. S. A. **96:**2408–2413.
50. **Towbin, H., T. Staehelin, and J. Gordon.** 1979. Electrophoretic transfer of proteins from polyacrylamide gels to nitrocellulose sheets: procedure and some applications. Proc. Natl. Acad. Sci. U. S. A. **76:**4350–4354.
51. **Wadhams, G. H., and J. P. Armitage.** 2004. Making sense of it all: bacterial chemotaxis. Nat. Rev. Mol. Cell. Biol. **5:**1024–1037.
52. **Whitchurch, C., S. Beatson, J. Comolli, T. Jakobsen, J. Sargent, J. Bertrand, M. Klausen, L. Waite, T. Tolker-Nielsen, P. J. Kang, J. Mattick, and J. N. Engel.** 2005. FimL, a novel *Pseudomonas aeruginosa* gene product involved in type IV fimbrial function and twitching motility. Mol. Microbiol. **55:**1357.

53. **Whitchurch, C. B., S. A. Beatson, J. C. Comolli, T. Jakobsen, J. L. Sargent, J. J. Bertrand, J. West, M. Klausen, L. L. Waite, P. J. Kang, T. Tolker-Nielsen, J. S. Mattick, and J. N. Engel.** 2005. *Pseudomonas aeruginosa fimL* regulates multiple virulence functions by intersecting with Vfr-modulated pathways. Mol. Microbiol. **55:**1357–1378.
54. **Whitchurch, C. B., M. Hobbs, S. P. Livingston, V. Krishnapillai, and J. S. Mattick.** 1991. Characterization of a *Pseudomonas aeruginosa* twitching motility gene and evidence for a specialized protein export system widespread in eubacteria. Gene **101:**33–44.
55. **Whitchurch, C. B., A. J. Leech, M. D. Young, D. Kennedy, J. L. Sargent, J. J. Bertrand, A. B. Semmler, A. S. Mellick, P. R. Martin, R. A. Alm, M. Hobbs, S. A. Beatson, B. Huang, L. Nguyen, J. C. Commolli, J. N. Engel, A. Darzins, and J. S. Mattick.** 2004. Characterization of a complex chemosensory signal transduction system which controls twitching motility in *Pseudomonas aeruginosa*. Mol. Microbiol. **52:**873–893.
56. **Whitchurch, C. B., and J. S. Mattick.** 1994. Characterization of a gene, *pilU*, required for twitching motility but not phage sensitivity in *Pseudomonas aeruginosa*. Mol. Microbiol. **13:**1079–1081.
57. **Winther-Larsen, H. C., and M. Koomey.** 2002. Transcriptional, chemosensory and cell-contact-dependent regulation of type IV pilus expression. Curr. Opin. Microbiol. **5:**173–178.
58. **Wu, S. S., and D. Kaiser.** 1997. Regulation of expression of the *pilA* gene in *Myxococcus xanthus*. J. Bacteriol. **179:**7748–7758.
59. **Zusman, D. R., A. E. Scott, Z. Yang, and J. R. Kirby.** 2007. Chemosensory pathways, motility and development in *Myxococcus xanthus*. Nat. Rev. Microbiol. **5:**862–872.